Human Molecular Genetics, 2011, Vol. 20, No. 2 **235–244**
doi:10.1093/hmg/ddq458
Advance Access published on October 14, 2010

Dystrophin conferral using human endothelium expressing HLA-E in the non-immunosuppressive murine model of Duchenne muscular dystrophy

Chang-Hao Cui[1,2], Shunichiro Miyoshi[3], Hiroko Tsuji[3], Hatsune Makino[1], Seiichi Kanzaki[1], Daisuke Kami[1], Masanori Terai[1], Harumi Suzuki[4] and Akihiro Umezawa[1,*]

[1]Department of Reproductive Biology, National Institute for Child Health and Development, Tokyo 157-8535, Japan, [2]Department of Basic Medical Science, Mudanjiang Medical College, Mudanjiang 157011, China, [3]Department of Cardiology, Keio University School of Medicine, Tokyo 160-8582, Japan and [4]Department of Pathology, Research Institute, International Medical Center of Japan, Tokyo 162-8655, Japan

Received July 13, 2010; Revised September 16, 2010; Accepted October 8, 2010

Human leukocyte antigen (HLA)-E is a non-classical major histocompatibility complex class I (Ib) molecule, which plays an important role in immunosuppression. In this study, we investigated the immunomodulating effect of HLA-E in a xenogeneic system, using human placental artery-derived endothelial (hPAE) cells expressing HLA-E in a mouse model. *In vitro* cell lysis analysis by primed lymphocytes in combination with siRNA transfection showed that HLA-E is necessary for inhibition of the immune response. Similarly, *in vivo* cell implantation analysis with siRNA-mediated down-regulation of HLA-E demonstrates that HLA-E is involved in immunosuppression. As hPAE cells efficiently transdifferentiate into myoblasts/myocytes *in vitro*, we transplanted the cells into mdx mice, a model of Duchenne muscular dystrophy. hPAE cells conferred dystrophin to myocytes of the 'immunocompetent' mdx mice with extremely high efficiency. These findings suggest that HLA-E-expressing cells with a myogenic potential represent a promising source for cell-based therapy of patients with muscular dystrophy.

INTRODUCTION

Duchenne muscular dystrophy (DMD) is a severe, recessive X-linked form of muscular dystrophy, characterized by rapid progression of muscle degeneration that eventually leads to loss in ambulation, paralysis and death. The disorder is caused by a mutation in the gene encoding dystrophin, an important structural component of muscle tissues. The absence of intact dystrophin results in destabilization of the extracellular membrane–sarcolemma–cytoskeleton architecture, making muscle fibres susceptible to contraction-associated mechanical stress and degeneration. Skeletal muscles degenerate progressively and irreversibly and are replaced by fibrotic tissues (1). Several protocols have been developed for cell-based therapies, especially using an mdx mouse model, in which mouse dystrophin is defective due to a single point mutation (2,3).

There is no known cure for DMD. However, use of stem cells or myogenic progenitors holds significant potential as an effective and suitable treatment. Myoblasts represent the natural first choice in cell-based therapy for skeletal muscle due to their intrinsic myogenic commitment. However, myoblasts recovered from muscular biopsies are poorly expandable *in vitro* and rapidly undergo senescence (1). Cells with myogenic potential are present in many other tissues, and these cells readily form skeletal muscle under favourable culture conditions (4). Indeed, cell-based therapy for damaged muscle tissue has already reached the clinical setting, with several types of cell populations being exploited (5,6). Experimental approaches to DMD using animal models have also been

*To whom correspondence should be addressed at: National Institute for Child Health and Development, 2-10-1, Okura, Setagaya, Tokyo 157-8535, Japan. Tel: +81 354947047; Fax: +81 354947048; Email: umezawa@1985.jukuin.keio.ac.jp

© *The Author 2010. Published by Oxford University Press.*
This is an Open Access article distributed under the terms of the Creative Commons Attribution Non-Commercial License (http://creativecommons.org/licenses/by-nc/2.5), which permits unrestricted non-commercial use, distribution, and reproduction in any medium, provided the original work is properly cited.

extensively investigated, using cells derived from bone marrow (7), synovial membrane (8) and menstrual blood (9).

In any cell-based therapy, donor cells are frequently rejected by recipients when transplanted in an allogeneic combination. Rejection is caused by a mismatch of the human leukocyte antigen (HLA). There are a large number of different alleles of each HLA, so a perfect match of all HLAs between donor cells and host cells is extremely rare. HLA-E, together with HLA-G and HLA-F, is a non-classical major histocompatibility complex class I (MHC Ib) molecule (10), which plays an important role in immunosuppression. Among Ib molecules, HLA-E exhibits a restricted pattern of expression in different cell types (11) and is a ligand of CD94/NKG2 receptors (12,13). The interaction of HLA-E with the inhibitory CD94/NKG2 receptor results in the inhibition of natural killer (NK) cell- and cytotoxic T lymphocyte-dependent lysis (12,14). Uteroplacental immune privilege systems utilize this immunosuppression through production of HLA-E, HLA-F and HLA-G in the uterus and the placenta.

In this study, we investigated the immunomodulating effect of HLA (class Ib) in a xenogeneic combination, using placenta-derived cells expressing HLA-E. Human placental artery-derived endothelial (hPAE) cells conferred dystrophin to myocytes of 'immunocompetent' mdx mice, a model of DMD, doing so with extremely high efficiency.

RESULTS

Derivation of hPAE cells

We successfully cultured a large number of hPAE cells obtained from placental arteries of five donors by the explant culture method (Fig. 1A; see Materials and Methods). hPAE cells with endothelium-like morphology (Fig. 1B) adhered to dishes and were regarded as being population doubling (PD) 0 at day 2. They continued to proliferate until PD 17 at day 20 (Fig. 1C). Cell proliferative capacity was assessed by calculating the total number of PDs (PD level or accumulative PDs) using the formula $\log_{10}$(total number of cells/starting number of cells)/$\log_{10}$ 2. Flow cytometric analysis revealed that hPAE cells were positive for CD29 (integrin b1), CD31 (PECAM-1), CD44 (Pgp-1/ly24), CD59, CD73, CD105 and CD166 (ALCAM) and negative for CD45, CD106 (VCAM-1) and CD117 (c-kit) (Fig. 1D and E). Almost all the cells were positive for the endothelial marker CD31 (97.7%), implying that the cells were of endothelial origin. Reverse transcriptase (RT)–polymerase chain reaction (PCR) analysis revealed that hPAE cells expressed the endothelial markers constitutively (Fig. 1F). Immunocytochemical analysis also indicated that the hPAE cells were positive for CD31 and von Willebrand factor (vWF) (Fig. 1G). We next tested whether hPAE cells would form an 'angiogenesis network' when plated on Matrigel. As shown in Figure 1H, culture of hPAE cells on extracellular matrix resulted in vascular tube formation within 6 h. hPAE cells with vascular tube formation were immunocytochemically positive for vascular endothelial growth factor (VEGF) (Supplementary Material, Fig. S1).

Expression of HLA-E in hPAE cells

Since non-classical MHC is involved in immune privilege (10,15), we investigated whether hPAE cells produce HLA-E after exposure to cytokines (16). hPAE cells started to express HLA-E after exposure to cytokines at the transcriptional level (Fig. 2A) and the protein level (Fig. 2B and C). Immunostaining showed that HLA-E was mainly localized in the cytoplasm (Fig. 2B, right). Western blot analysis using anti-HLA-E-specific monoclonal antibody revealed a single discrete band at 42 kDa, consistent with the molecular weight of HLA-E protein (Fig. 2C). Immunoprecipitation analysis of the cell supernatant showed a single band at 37 kDa, consistent with the molecular weight of soluble HLA-E (sHLA-E) protein (Fig. 2D), implying that sHLA-E is secreted.

Myogenic induction of hPAE cells *in vitro*

We then investigated whether hPAE cells are capable of differentiating into skeletal myocytes *in vitro* (Fig. 3). hPAE cells started to exhibit multinucleated myotubes in culture after induction (Fig. 3A). Immunocytochemistry indicated that enhanced green fluorescent protein (EGFP)-labelled multinucleated myotubes were positive for desmin (Fig. 3B) and myosin heavy chain (Fig. 3C and D). Myogenesis of hPAE cells was also analysed by RT–PCR with primers that can amplify human myogenic genes, but not their mouse counterparts. hPAE cells constitutively expressed the myogenin gene and started to express the desmin and MyHC-IIx/d genes after induction (Fig. 3E). We also performed tartrate-resistant acid phosphatase stain for osteoclasts, alkaline phosphatase stain for osteoblasts and Oil red O stain for adipocytes on hPAE cells at 21 days after the start of co-cultivation (Supplementary Material, Fig. S2), but failed to detect positive reaction by these stains.

Direct implantation of hPAE cells into immunocompetent BALB/c mice

To further evaluate the *in vivo* response to hPAE cells, cells were directly injected into the thigh muscles of immunocompetent BALB/c mice (17). For comparison, periosteal cells with low expression of HLA-E were injected in the same manner. Histopathological analysis revealed that the injection of periosteal cells induced an immune response at the injected site (Fig. 4A), but hPAE cells did not (Fig. 4B), suggesting that hPAE cells fail to elicit pro-inflammatory responses in immunocompetent mice. Immunohistochemical analysis, using an antibody specific to human vimentin, revealed that the hPAE cells extensively migrated between muscular fibres (Fig. 4B, lower panels). Immunofluorescent analysis revealed that CD45 and CD3 lymphocytes infiltrated near the (donor) periosteal cells at 2 days after the injection into the Balb/c muscle, and the number of lymphocytes increased at 2 weeks (Fig. 4C). In contrast, CD45- and CD3-positive cells were not detected around the vimentin-positive hPAE cells at 2 weeks. We also performed immunofluorescent analysis and western blot analysis to investigate the expression of HLA-E *in vivo*. hPAE cells expressed HLA-E in the muscle tissues (Fig. 4D and E). Moreover, HLA-E expression

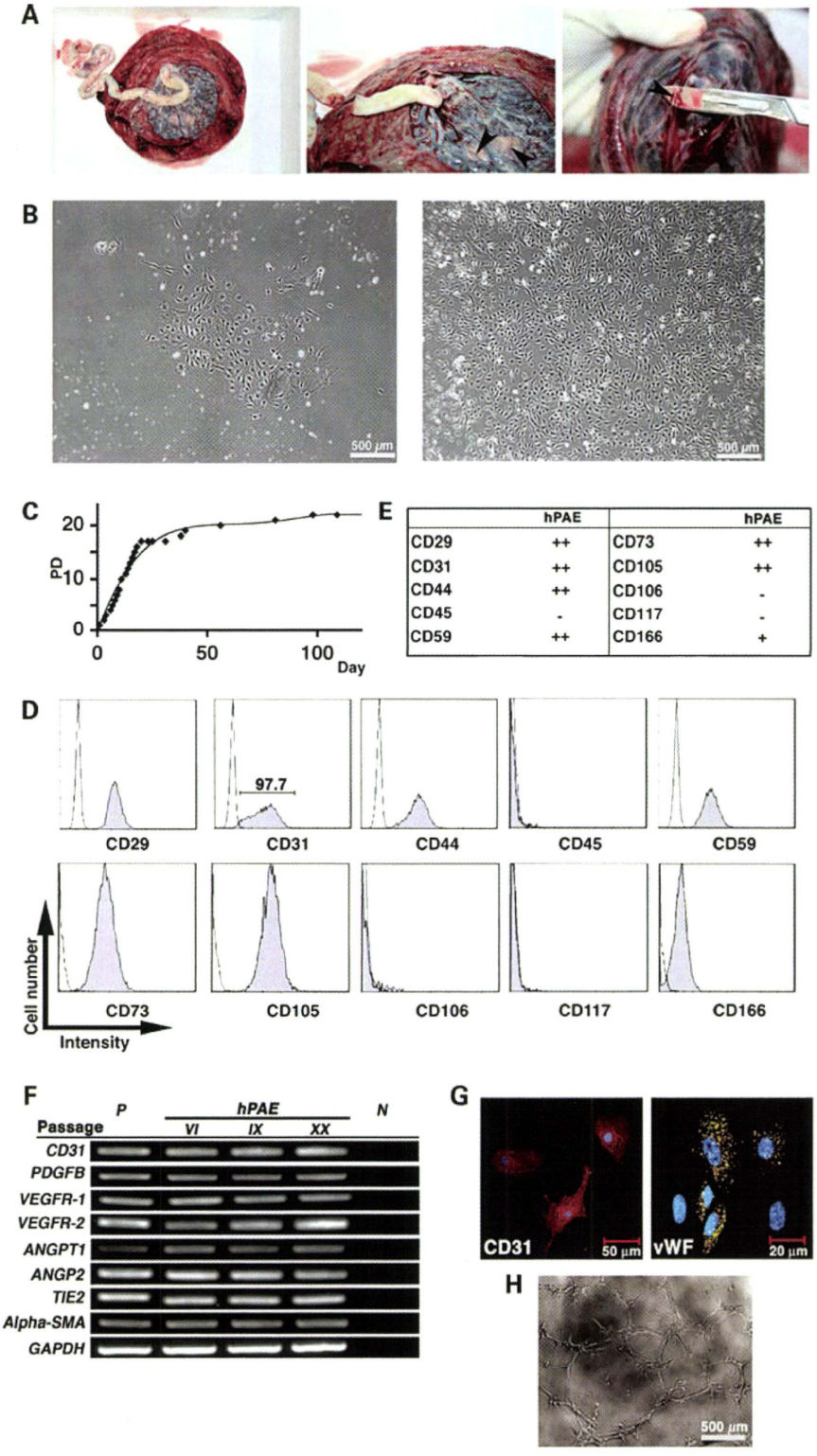

Figure 1. *In vitro* characterization of hPAE cells. (**A**) Macroscopic views showing an explant culture method of hPAE cells. hPAE cells were dissected from isolated placenta arterial vessels (indicated by arrowheads) in human placenta. (**B**) Photos showing morphology of hPAE cells by phase contrast microscopy at primary stages at passage I (left panel: PD 0 and right panel: PD 3). (**C**) Proliferative capacity of hPAE cells. The number of cells was counted with ViCell (Beckman Coulter) at each passage. The total number of PDs (PD level or accumulative PDs) was calculated, using the formula $\log_{10}$(total number of cells/starting number of cells)/$\log_{10}$ 2. (**D**) Flow cytometric profiles indicating expression of several cell surface markers on hPAE cells. (**E**) Scores of peak intensity, compared with isotype controls. '++': strongly positive (10 times and above that of the isotype control), '+': weakly positive (<10 times and twice and above that of the isotype control), '−': negative (less than twice that of the isotype control). (**F**) RT–PCR analysis for endothelial marker expression in hPAE cells at passage VI, IX and XX. The cells were cultured without any inductive stimuli. RNAs from HUVECs and H_2O serve as positive (P) and negative (N) controls, respectively. (**G**) Immunocytochemical analyses of CD31 and vWF in hPAE cells. (**H**) Phase contrast micrograph of *in vitro* endothelial network formation of hPAE cells. hPAE cells were cultured on a basement membrane matrix gel. An 'angiogenesis network' was formed 6 h after cultivation began.

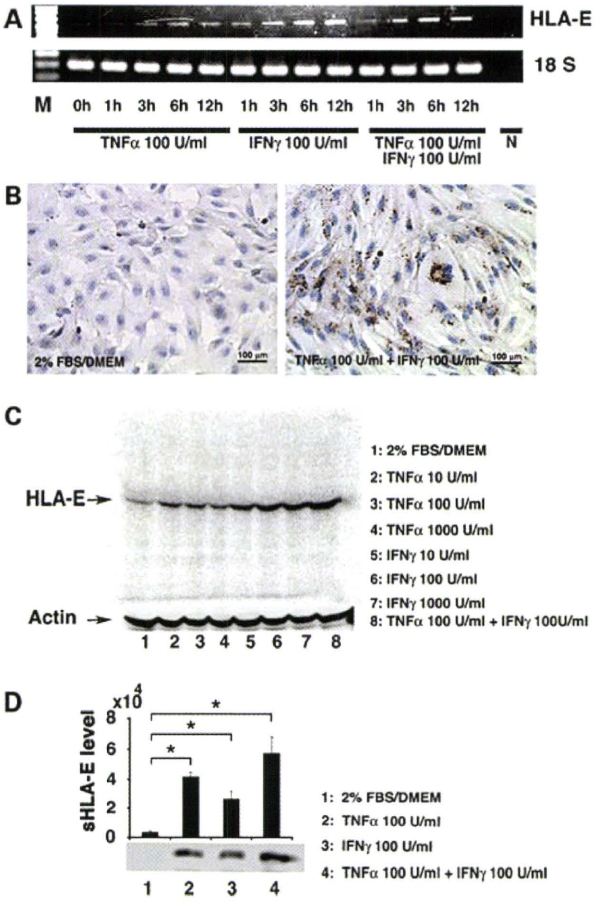

Figure 2. HLA-E mRNA and protein in hPAE cells upon treatment with tumor necrosis factor α (TNFα) and interferon γ (IFNγ). (**A**) RT–PCR showing a time-course of HLA-E expression in response to TNFα and IFNγ. 18S RNA was used as a loading control. M = size markers and N = a negative control in PCR with H_2O. (**B**) Immunocytochemistry of HLA-E localization. The cells were incubated for 24 h with a combination of TNFα and IFNγ at the indicated concentrations (right). Left panel = untreated control. (**C**) Western blot analysis of cell lysates showing levels of HLA-E at 24 h after treatment with TNFα and IFNγ. Combination of two reagents induced more HLA-E at the protein level. Actin was used as a loading control. (**D**) Immunoprecipitation analysis of culture supernatants showing a soluble form of HLA-E (sHLA-E) with exposure to TNFα and IFNγ. sHLA-E level was determined by each signal intensity (mean ± SE). $n = 3$, $^*P < 0.05$.

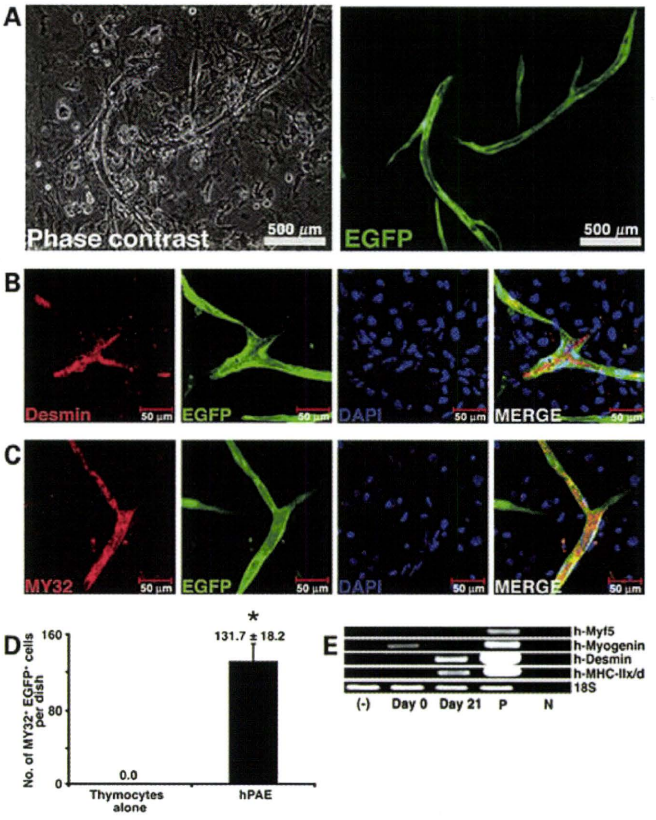

Figure 3. Myogenic differentiation of hPAE cells under cell culture conditions. (**A**) Photos showing myogenic differentiation of hPAE cells detected by phase contrast microscopy (left) and by fluorescent microscopy (right) in an identical area. EGFP-labelled hPAE cells co-cultured with neonatal murine thymocytes for 21 days. (**B** and **C**) Immunocytochemistry of hPAE cells expressing myogenic markers, desmin (B) and skeletal myosin heavy chain (C, MY32). (**D**) Quantitative analysis of MY32-positive hPAE cells. MY32- and EGFP-double positive cells (no. of MY32+ EGFP+ cells) were counted in 35 mm dishes 3 weeks after induction (mean ± SE). $n = 3$, $^*P < 0.05$. (**E**) RT–PCR showing myocyte-specific genes were expressed along with myogenic differentiation. RT–PCR analysis with PCR primers that amplify only human mRNAs of Myf5, myogenin, desmin and MyHC-IIx/d, but not murine mRNAs. RNAs from human muscle and H_2O served as positive (P) and negative (N) controls, respectively.

remained unchanged over 6 weeks. We then examined interleukin-4 (IL-4), which is essential for transplantation immunity. IL-4 production reached a maximum level after 2 weeks at the injected site and then decreased (Supplementary Material, Fig. S3).

To investigate whether hPAE cells can generate muscle tissue *in vivo*, hPAE cells were implanted directly into the right thigh muscles of BALB/c mice, with phosphate-buffered saline (PBS) being injected at the contralateral muscles as a control. Immunohistochemical analysis was performed using the human-specific antibody at 3 weeks after injection. Myotubes at the injected site expressed human dystrophin as a cluster. No positive reaction was detected in the muscle of BALB/c mice without cell implantation (PBS alone) (Fig. 4E and F; Supplementary Material, Fig. S4). These results imply that dystrophin is transcribed from the dystrophin gene of human donor cells after hPAE cells differentiated into myotubes and fused to host myocytes without immune response. To determine whether human dystrophin expression in the donor cells is caused by fusion, immunohistochemistry with an antibody against human nuclei (Ab-HuNucl) and 4′,6-diamidino-2-phenylindole (DAPI) stain was performed. We examined almost all the 7 mm thick serial histological sections parallel to the muscular bundle (cross-section) of the muscular tissues by confocal microscopy and found that myocytes had nuclei derived from both human and murine cells in the cross-section (Fig. 4G), implying that dystrophin expression is attributed to fusion between murine host myocytes and human donor cells.

Inhibition of HLA-E by small interfering RNA (siRNA)

To investigate the involvement of HLA-E in immunosuppression, we suppressed HLA-E expression by siRNA in hPAE cells. A significant decrease in HLA-E mRNA was observed

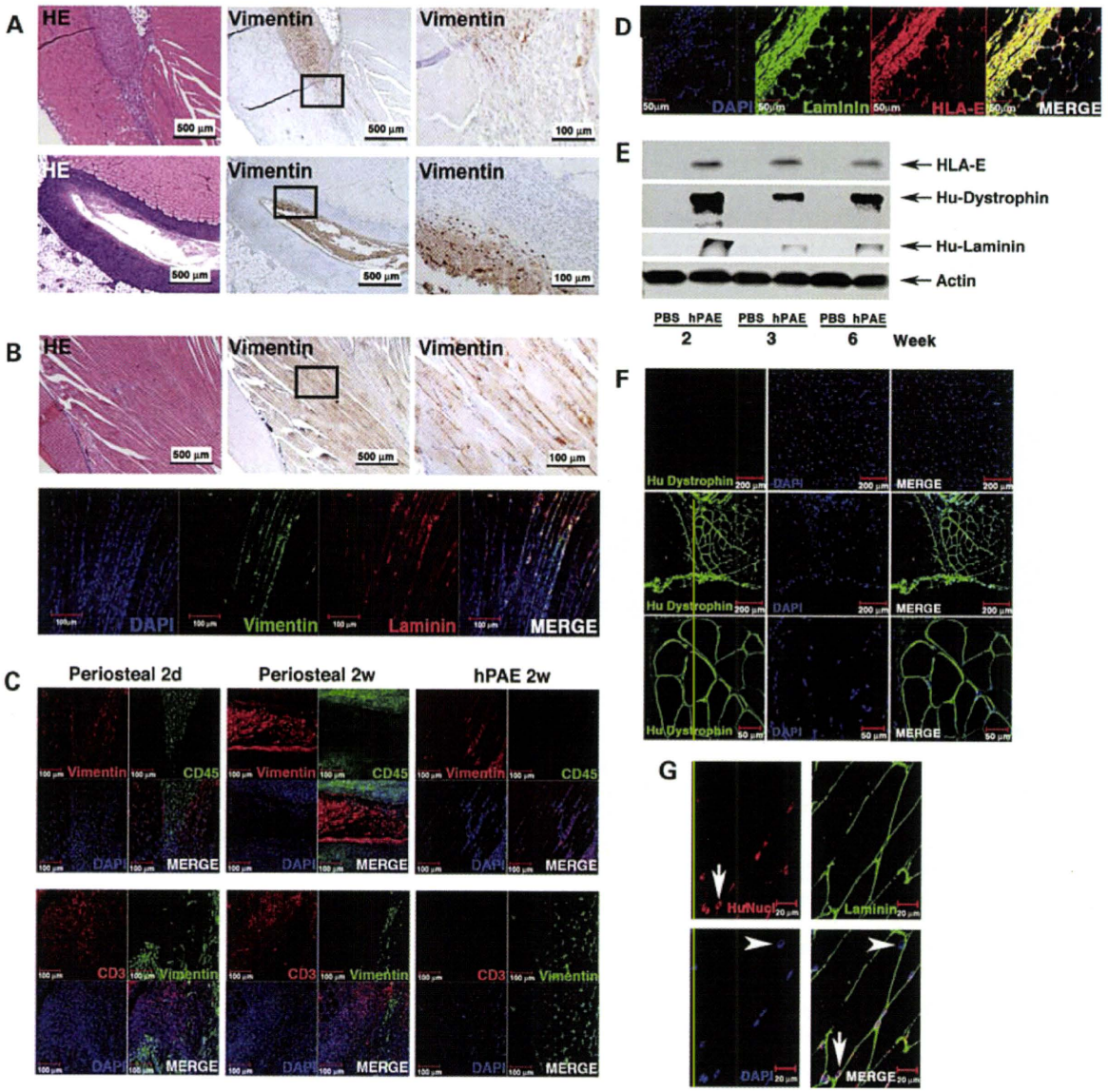

Figure 4. Implantation of hPAE cells into the thigh muscle of BALB/c mice. (**A**) Human periosteal cells (2×10^7 cells) were injected directly into the thigh muscles of BALB/c mice. Immunohistochemical analysis was performed on the muscle section using an antibody against vimentin. Upper panels: 2 days after injection and lower panels: 2 weeks after injection. (**B**) hPAE cells (2×10^7 cells) were injected directly into the thigh muscles of BALB/c mice. Upper panels: immunohistochemistry against vimentin. Lower panels: immunofluorescent analysis. DAPI (blue), vimentin (green), laminin (red) and MERGE (from left to right). (**C**) Immunohistochemical analysis of the thigh muscle sections at 2 days or 2 weeks after injection of human periosteal cells (hPeriosteal) and at 2 weeks after injection of hPAE cells, using antibodies against vimentin (upper panels: red and lower panels: green), leukocyte marker CD45 (green) and T cell marker CD3 (red). (**D**) Immunofluorescent analysis using an antibody against HLA-E (red) and human laminin (green) on the thigh muscle sections at 2 weeks after injection of hPAE cells. (**E**) Western blot analysis of muscle lysates showing levels of HLA-E, dystrophin and laminin. BALB/c mice were implanted with PBS or hPAE cells at the indicated weeks. The level of actin protein was used as a loading control. (**F**) Immunofluorescent analysis using an antibody against human dystrophin (green) on thigh muscle sections 3 weeks after direct injection of hPAE cells (middle and lower panels). PBS was injected into contralateral muscles as a control (upper panels). Dystrophin is totally absent in PBS-injected muscles (upper panels), whereas clusters of muscle fibres display peripheral localization of the dystrophin protein in mice injected with hPAE cells (middle and lower panels). Dystrophin (green), DAPI (blue) and MERGE (from left to right). (**G**) Immunofluorescent analysis using antibodies against laminin (green), human nuclei (HuNucl, red, arrows) and DAPI staining (blue, arrowheads) on thigh muscle sections 3 weeks after injection of hPAE cells.

in the cells transfected with HLA-E siRNA (siHLA-E) when compared with control cells (Fig. 5A). In the same set of experiments, HLA-E protein decreased significantly in siHLA-E-transfected cells when compared with control cells (Fig. 5B). To investigate the involvement of HLA-E in *in vivo* immune response, after pre-treatment with 20 μM siHLA-E for 48 h, hPAE cells were injected into the thigh muscles of immunocompetent BALB/c mice, with hPAE cells treated with control siRNA being injected into the contralateral muscles as a control (Fig. 5C–F). Histopathological analysis revealed that injection of siHLA-E-treated hPAE cells elicited an immune response, as revealed by infiltration of CD3- and CD45-positive lymphocytes in immunocompetent BALB/c mice 7 days after injection, whereas injection of

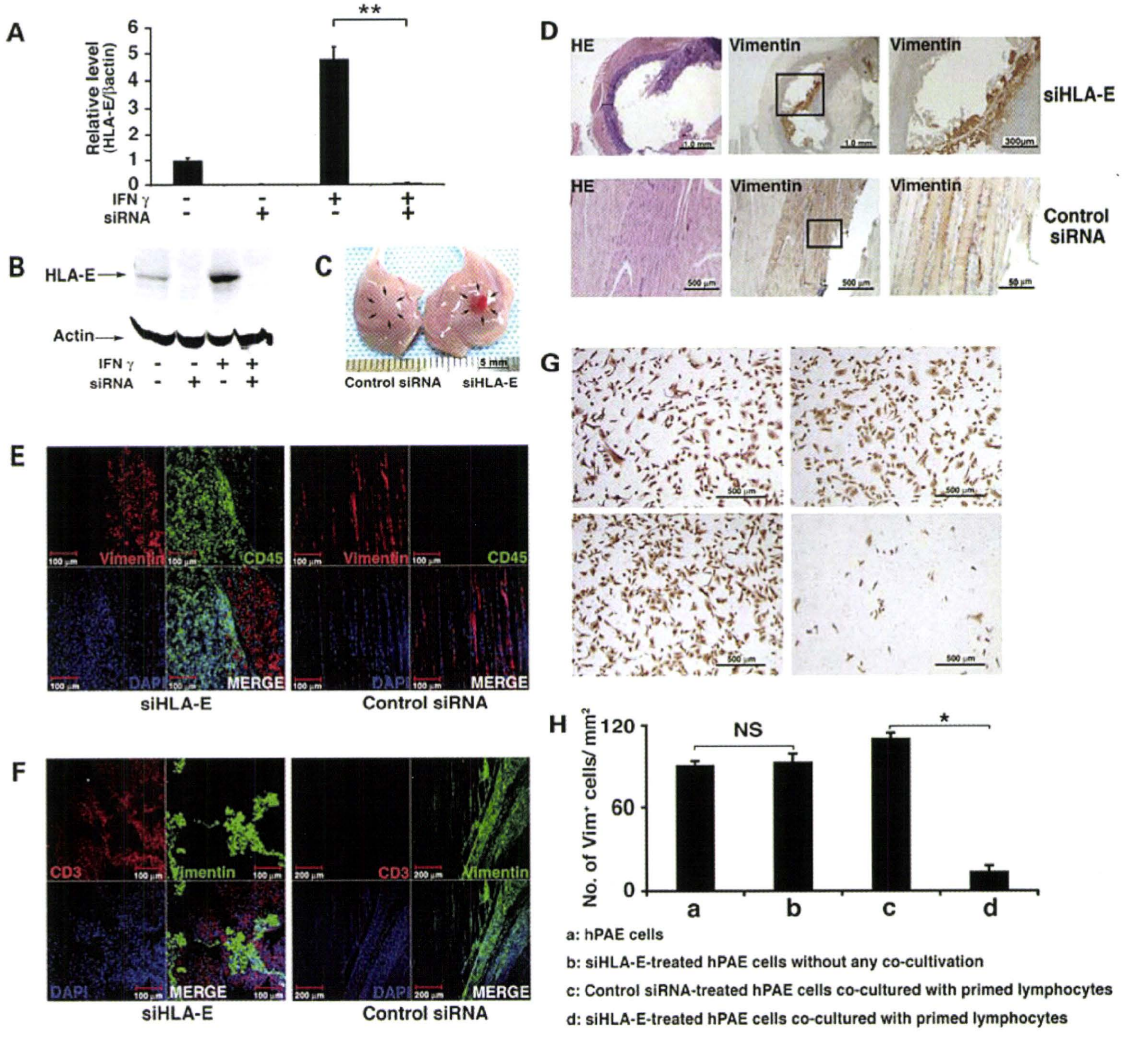

Figure 5. Functional effect of HLA-E siRNA on immunosuppression. (**A**) Inhibition of HLA-E mRNA by siRNA. hPAE cells (1×10^4) grown on 6-well plates were transfected with either control siRNA or HLA-E-specific siRNA (20 μM) for 48 h. HLA-E mRNA levels were quantified using RT–PCR, normalized to β-actin (mean ± SE). $n = 3$, $^{**}P < 0.01$. (**B**) Inhibition of HLA-E protein by siRNA. Whole-cell protein extracts were analysed by SDS–PAGE immunoblotting with antibodies to HLA-E and actin. (**C**–**F**) siHLA-E-treated hPAE cells and control siRNA-treated hPAE cells were injected into the right and left thigh muscle of BALB/c mice, respectively. Mice were sacrificed 7 days after injection. (C) Injected sites are indicated by arrows (left: control siRNA and right: HLA-E-specific siRNA). (D) Microscopic view (HE stain and immunohistochemistry) of thigh muscles implanted with siHLA-E-treated (upper panels) or control siRNA-treated (lower panels) hPAE cells. (E and F) Immunohistochemical analysis of thigh muscle sections, after injection of siHLA-E-treated or control siRNA-treated hPAE cells and staining with antibodies against vimentin (E: red and F: green), leukocyte marker CD45 (E: green) and T cell marker CD3 (F: red). (**G**) Induction of xenoreactive lysis with spleen-derived lymphocytes. siHLA-E-treated hPAE cells or control siRNA-treated hPAE cells were co-cultured with spleen-derived lymphocytes and immunocytochemically stained for human vimentin. (G) Upper left: hPAE cells, upper right: siHLA-E-treated hPAE cells without any co-cultivation, lower left: control siRNA-treated hPAE cells co-cultured with primed lymphocytes, lower right: siHLA-E-treated hPAE cells co-cultured with primed lymphocytes. (**H**) Survival of hPAE cells after xenoreactive analysis. Vimentin-positive cells (no. of vimentin+ cells/mm^2) significantly decreased in siHLA-E-treated cells when compared with control siRNA-treated cells 3 days after co-incubation with primed lymphocytes. $^*P < 0.01$, NS = not significant.

control siRNA-treated hPAE cells did not (Fig. 5E and F). This suggests that HLA-E is necessary for inhibition of an immune reaction *in vivo*. We then investigated whether lysis of hPAE cells by primed lymphocytes is mediated by HLA-E. hPAE cells treated with either siHLA-E or control siRNA were co-cultured with spleen-derived lymphocytes, and induction of xenoreactive lysis was quantified (Fig. 5G and H). siHLA-E-treated hPAE cells were lysed by primed lymphocytes, whereas control siRNA-treated hPAE cells were not, indicating that HLA-E is also necessary for inhibition of the immune response *in vitro*.

Conferral of human dystrophin by cell implantation in the mdx mouse

To investigate whether hPAE cells can confer human dystrophin to myocytes, untreated EGFP-labelled cells were implanted directly into the thigh muscles of mdx mice (Fig. 6A). PBS was injected into the contralateral muscles as a control (Fig. 6B). At 3 weeks after implantation, human dystrophin was detected in EGFP-positive myotubes as a cluster at 18.2% (Fig. 6C). Expression of dystrophin was not caused by reversion to the normal phenotype of dystrophied myocytes

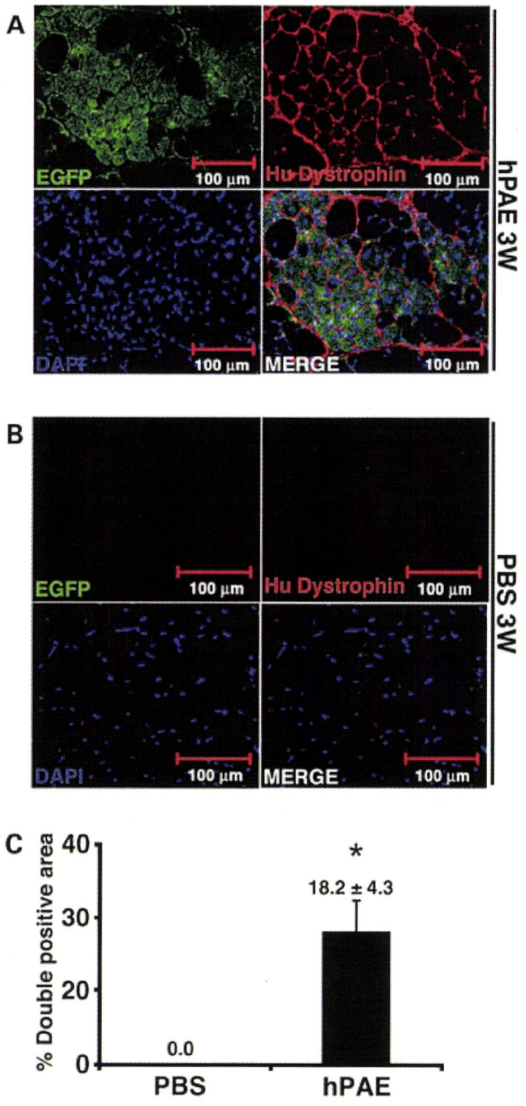

Figure 6. Conferral of dystrophin to mdx myocytes by hPAE cells. (**A**) EGFP-labelled hPAE cells were injected into the thigh muscle of mdx mice. Immunohistochemical analysis revealed the incorporation of implanted cells into newly formed EGFP-positive myofibres (green), which expressed human dystrophin (red) 3 weeks after implantation. (**B**) PBS was injected into contralateral muscles as a control. (**C**) Quantitative analysis of human dystrophin-positive myotubes. The percentage of human EGFP- and dystrophin-positive myofibre areas (% double positive area) was calculated 3 weeks after injection of cells or PBS (mean ± SE). $n = 3$, $^*P = 0.05$.

in the mdx mice because the antibody used in this study is specific to humans. These results suggest that human dystrophin is transcribed from the dystrophin gene of human donor cells.

DISCUSSION

DMD is a devastating X-chromosome-linked muscle disease characterized by progressive muscle weakness attributable to a lack of dystrophin expression at the sarcolemma of muscle fibres (18). There are currently no effective therapeutic approaches for muscular dystrophy. hPAE cells have a high replicative ability, similar to progenitors or stem cells that display a long-term self-renewal capacity, and had a much higher growth rate in our experimental conditions than marrow-derived stromal cells (19). Immunosuppressive hPAE cells with a direct myogenic potential thus offer significant potential for novel, effective and sustainable cell-based therapy, including when being used in an allogeneic manner. The function of HLA-E has been fully elucidated through its interaction with CD94-NKG2 receptors expressed on NK cells and a subset of T cells (12,13). *In vitro* studies using human cells provided evidence of HLA-E involvement in negative signalling to immune responses (20). Qa-1 (homologous to HLA-E in mice)-deficient mice have defects in immunoregulation mediated by T cells (21). Survival of donor cells in an immunocompetent mouse is attributed, at least partially, to HLA-E-dependent immunosuppression, because knockdown experiments of HLA-E clearly indicate involvement of HLA-E in cell-mediated lysis of hPAE cells (Fig. 5). HLA-E is a protective response of hPAE cells to injury and plays an important role in immunosuppression, irrespective of being either the membrane-bound or soluble form.

It is noteworthy that hPAE cells, as well as other placenta-derived cells, are obtained by a simple, safe and painless procedure, and a large number of hPAE cells can easily be harvested from placental arteries. In this study, we manually separated chorionic large arteries from the chorionic plate that entirely covers the foetal surface of the placenta, which is, in turn, covered by the aminion (Fig. 1A). hPAE cells proliferate over at least PD 17 for >20 days and stop dividing before PD 22. The predicted number of CD31-positive hPAE cells from one placenta of an average size (500 g) would be 1×10^7 (before *ex vivo* amplification), possibly reaching 1×10^{12} after cultivation. This may cover 30 000 cm^3 of muscular tissues in cell-based therapy (5). Cells converted into myotubes *in vitro* at a high frequency after induction, giving rise to large numbers of myofibres expressing human dystrophin when transplanted into BALB/c and mdx mice, thus fulfilling all the criteria required for a successful allogeneic cell therapy for muscular dystrophy.

Compared with previously reported experiments, including from our laboratory (9), the frequency of myotubes with human dystrophin after cell implantation was extremely high. In addition to *in vivo* myogenesis, *in vitro* myogenesis was induced. Myogenin, a helix–loop–helix transcription factor, determines muscle cell fate and accelerates cell fusion, and is constitutively expressed in hPAE cells, implying either that these cells have myogenic potential or that these cells are myogenic progenitors, although their origin is endothelial from the viewpoint of isolation procedure and cell surface markers. Myogenesis may also be promoted by cytokines such as VEGF (22) as well as transcription factors. Furthermore, in cases of cell-based therapy, the so-called 'space' is necessary for survival of implanted donor cells. Irradiation has been used for the generation of space in cases of bone marrow transplantation. Toxin, to induce muscle injury and pathophysiological ischaemia of muscular tissues, can also generate space in muscle (23). BALB/c and mdx mice were used in this study, and almost identical results were obtained from both mice types, although BALB/c mice theoretically do not have any muscular injury. High frequency of human

dystrophin-positive myotube formation may be attributed to the generation of space by the immune response after cell implantation in a xenogeneic combination. hPAE cells produce HLA-E after immunoreaction by production of immunocytokines such as IL-4 (Supplementary Material, Fig. S1), followed by induction of immunosuppression through HLA-E. This immune reaction after cell implantation possibly generates space to enable survival of implanted cells. This possibility is rather favourable because any future cell-based therapy for DMD patients will be employed in an allogeneic combination. In contrast, experimental approaches have been tested in a syngeneic combination, in immunodeficient mice or via use of immunosuppressive drugs. Clinical trials in humans, use an allogeneic combination (5,6), are in no way inferior compared with experimentation with the murine model systems. This study may explain the high frequency of donor cell survival at the implanted sites observed in clinical trials.

Induction of immunosuppression via HLA-E from hPAE cells observed in this study directly leads to the possibility of clinical, allogeneic cell-based therapy. Mesenchymal stem cells (MSCs) or mesenchymal progenitors, isolated from bone marrow as an adherent fibroblast-like population (24), have already been identified in many tissues, including umbilical-cord blood (25), the placenta (26), fat and amniotic fluid (27). They have been used for cell-based therapy because of their self-renewal capacity and their ability to form bone, fat, cartilage, muscle, cardiocytes and neurons (28,29). The isolation of tissue-specific stem cells for expansion *in vitro* and transplantation back into the patient in an allogeneic manner is an ideal strategy, from the viewpoint of industry-based, sustainable supply of large quantities of affordable, quality-controlled cells. Using autologous MSCs to restructure damaged tissues has had some clinical success (30). In most cases of degenerative and genetic diseases, it is unlikely that enough unaffected stem cells will be isolated or available in sufficient quantity, necessitating the use of stem cells from suitable, cost-effective allogeneic sources such as placenta.

MATERIALS AND METHODS

Cultivation of hPAE cells

Human placentas were collected, after delivery, with informed consent. Ethical approval was granted by the Institutional Review Board. To isolate arterial endothelium, we used the explant culture method, in which the cells were outgrown from pieces of placenta arterial vessels (Fig. 1A). Briefly, arterial vessels were separated from arteries in the chorionic plate and chopped into $\sim 5\ mm^3$ pieces. The pieces were washed in endothelial basal medium (EBM)-2 (Cambrex, Walkersville, MD, USA) and cultured in endothelial growth medium-2 MV (EGM-2MV; Cambrex), which consisted of EBM-2, 5% foetal bovine serum (FBS) and supplemental growth factors including VEGF, basic fibroblast growth factor, epidermal growth factor and insulin-like growth factor. Arterial vessels attached to the substratum of culture dishes (BD Falcon; Becton Dickinson and Company, San Jose, CA, USA), and cells migrate out from the surface of tissues after 20 days of incubation at 37°C in 5% CO_2. The cells were harvested with PBS, with 0.1% trypsin and 0.25 mM EDTA, and were re-seeded at a density of 3×10^5 cells in a 10 cm diameter dish. Confluent monolayers of cells were further subcultured. The culture medium was replaced every 3–4 days.

In vitro lentivirus-mediated gene (EGFP) transfer into hPAE cells

Infection of cultured hPAE cells with lentivirus (having a CMV promoter-regulated EGFP reporter plasmid) resulted in high levels of EGFP expression in all cells. EGFP expression was analysed by flow cytometry (31).

Flow cytometric analysis

Flow cytometric analysis was performed as described previously (9). Cells were incubated with primary antibodies or isotype-matched control antibodies followed by immunofluorescent secondary antibody staining. Cells were analysed on an EPICS ALTRA analyser (Beckman Coulter, Fullerton, CA, USA). Antibodies against human CD29, CD31, CD44, CD45, CD59, CD73, CD105, CD106, CD117, CD166 and VEGER (FIk-1) were purchased from Beckman Coulter, Immunotech (Marseille, France), Cytotech (Hellebaek, Denmark) and BD Biosciences Pharmingen (San Diego, CA, USA).

Myogenic differentiation of hPAE cells

A cell suspension was prepared from neonatal murine thymi using frosted slide glasses (MUTO-Glass, Japan). The thymocyte suspension was then washed once in PBS with 2% FBS and filtered through a 100 μm nylon mesh. After centrifugation at 1000 rpm for 5 min, the cell pellet was re-suspended in 10% FBS/Dulbecco's modified Eagle's medium. Floating thymocytes were collected and re-plated at $1 \times 10^6/cm^2$. The next day, hPAE cells were harvested with 0.25% trypsin and 1 mM EDTA and overlaid onto the cultured neonatal thymocytes at $1 \times 10^4/cm^2$. The culture medium was replaced every 2 days with fresh EGM-2 MV.

RT–PCR analysis

Total RNAs (2 μg) were reverse-transcribed with oligo (dT), as described previously (9), and RT–PCR was carried out with primer sets specific for human Myf5, myogenin, desmin, myosin heavy chain-IIx/d (MyHC-IIx/d) (primer sequences are shown in Supplementary Material, Table S1). Human muscle RNAs and H_2O served as positive (P) and negative (N) controls, respectively. The 18S PCR primers were used as a positive control for both human and murine cDNAs. The HLA-E primers (F: CCACCATGGTAGATG GAACCC and R: GCTTTACAAGCTGTCAGACTC) used were the same as those described previously (16). The primer sequences of endothelial cell markers are listed in Supplementary Material, Table S1. Human umbilical vein endothelial cell (HUVEC) RNAs and H_2O served as positive (P) and negative (N) controls, respectively. Glyceraldehyde phosphate dehydrogenase was also used as a positive control.

For quantitative analysis of mRNA levels for HLA-E, the total RNAs were isolated from HLA-E-specific siRNA or control siRNA-transfected hPAE cells using an RNeasy mini-kit (Qiagen, Chatsworth, CA, USA) and were reverse-transcribed by TaKaRa recombinant Taq (Takara Bio Inc., Japan). Real-time PCR was carried out with an ABI PRISM 7000 Sequence Detection System. The 25 μl reaction mixture contained 12.5 μl of SYBR Green PCR Master Mix (TOYOBO, Japan), 10 ng of cDNA template and a primer set for HLA-E, F: CGGCTACTACAATCAGAGCGA and R: CACGCATGTGTCTTCCAGG or for β-action, F: CATGTACGTTGCTATCCAGGC and R: CTCCTTAATGTCACGCACGAT. The relative quantification of the transcripts was analysed using the comparative threshold cycle method supplied by the manufacturer.

Immunohistochemical and immunocytochemical analyses

For immunohistochemical analysis (19), the skeletal muscle tissue section slides (paraffin-embedded) were incubated with anti-vimentin monoclonal antibody (clone: V9, Dakocytomation, Glostrup, Denmark) for 1 h at room temperature, followed by horseradish peroxidase (HRP)-conjugated secondary antibody. Staining was detected by diaminobenzidine and H_2O_2. Slides were counterstained with haematoxylin. For the immunofluorescence, antibodies against human dystrophin (NCL-DYS3, Novocastra, Newcastle upon Tyne, UK), GFP (Catalogue no. 632377, Clontech, Mountain View, CA, USA), human nuclei (Catalogue no. MAB1281, Chemicon, Temecula, CA, USA), HLA-E (clone 4D12, MBL, Japan), vimentin, CD45 (leukocyte common antigen) (clone 30-F11, Invitrogen, Camarillo, CA, USA), CD3 (Catalogue no. sc-1127, Santa Cruz Biotechnology, Santa Cruz, CA, USA) and laminin (Mob 202, clone 4C7, DBS, CA, USA; 4H8-2, ab11576, Abcam plc, Cambridge, UK) were used as first antibodies, followed by Alexa-Fluor-conjugated secondary antibodies (Molecular Probes, Eugene, OR, USA).

Immunocytochemical analysis was performed as described previously (19). The antibodies against CD31 (Catalogue no. SCR023, Part no. 2003788, Chemicon), vWF (Catalogue no. SCR023, Part no. 2003787, Chemicon), VEGF (clone EP1176Y, Abcam plc), desmin (clone D9, Catalogue no. 010031, BioScience Products, Emmenbruecke, Switzerland), skeletal myosin (clone MY-32, Sigma-Aldrich, Inc., St Louis, MO, USA), GFP and vimentin were used as first antibodies and Alexa-Fluor-conjugated goat anti-mouse (rabbit) IgG and HRP-conjugated rabbit anti-mouse IgG were used as second antibodies.

Western blotting and immunoprecipitation

Western blot analysis was performed as described previously (19). Blots were incubated with primary antibodies for HLA-E (clone MEM-E/02, Serotec, Oxford, UK), laminin (Mob 202, clone 4C7, DBS) or dystrophin (NCL-DYS3, Novocastra) for 1–2 h at room temperature. After washing, blots were incubated with an HRP-conjugated secondary antibody (0.04 μg/ml) for 30 min. The blots were developed with enhanced chemiluminescence substrate, according to the manufacturer's protocol.

For immunoprecipitation, the supernatants of hPAE cell were incubated with HLA-E antibody (1–2 μg for each sample) for 1 h, followed by incubation with 20 μl of protein A/G plus agarose overnight at 4°C. The supernatants were removed by centrifugation, and the pellets were boiled in 2× sample buffer for 4 min. The products were then applied to sodium dodecyl sulphate (SDS)–polyacrylamide gel electrophoresis (PAGE).

siRNA study

The HLA-E siRNA pool (HLA-E-HSS104836, HLA-E-HSS104837 and HLA-E-HSS104838) was purchased from Invitrogen (Carlsbad, CA, USA) and transfected into hPAE cells using Lipofectamine™ RNAiMAX (Invitrogen). Cells were harvested 48 h after transfection and analysed by real-time PCR and western blot.

Xenoreactive immune response

Lymphocytes from BALB/c mouse spleen were isolated by Ficoll/Histopaque density gradient centrifugation. hPAE cells were transfected with either control siRNA or HLA-E-specific siRNA (20 μM) for 48 h. The two cell populations were then co-cultured for 3 days in 2 ml of RPMI supplemented with 10% FBS and 10 U/ml IL-2 (Catalogue no. 212-12, Peprotech Inc., Rocky Hill, NJ, USA). Induction of xenoreactive lysis in the spleen-derived lymphocytes was quantified by immunostaining with a human-vimentin-specific antibody.

In vivo cell implantation

hPAE cells were implanted into the thigh muscle of 4- to 6-week-old BALB/c (Sankyo Labo Service Corporation, Hamamatsu, Japan) or mdx (C57BL/10ScSn-Dmdmdx/J, Jax Labs, Bar Harbor, ME, USA) mice. For comparison, human periosteal cells were used. The cells (2×10^7) were suspended in PBS in a total volume of 100 μl and injected directly into the thigh muscles. The mice were examined 2 days or 1, 2, 3, 4 and 6 weeks after injection by immunohistochemistry with antibodies against HLA-E, vimentin, laminin and dystrophin. The antibodies for vimentin and dystrophin (NCL-DYS3) are human tissue specific; therefore, they do not react with murine tissues or murine tissue-derived proteins. In addition, siHLA-E (20 μM)-treated or control siRNA-treated hPAE cells were injected directly into the thigh muscle of BALB/c mice.

Statistical analysis

Statistical analysis was performed using the Student's *t*-test. A 95% confidence limit was taken as significant.

SUPPLEMENTARY MATERIAL

Supplementary Material is available at *HMG* online.

ACKNOWLEDGEMENTS

We would like to express our sincere thanks to M. Yamada for fruitful discussion and critical reading of the manuscript, H. Abe for providing expert technical assistance and to K. Saito for secretarial work.

Conflict of Interest statement. None declared.

FUNDING

This work was supported by Grants-in-Aid from the Japan Society for the Promotion of Science (21659092 and 22616011) and the Intramural Research Grant (19B-7 and 22-5) for Neurological and Psychiatric Disorders of NCNP. Funding to pay the Open Access publication charges for this article was provided by the Intramural Research Grant (22-5) for Neurological and Psychiatric Disorders of NCNP.

REFERENCES

1. Cossu, G. and Mavilio, F. (2000) Myogenic stem cells for the therapy of primary myopathies: wishful thinking or therapeutic perspective? *J. Clin. Invest.*, **105**, 1669–1674.
2. Hoffman, E.P., Brown, R.H. Jr and Kunkel, L.M. (1987) Dystrophin: the protein product of the Duchenne muscular dystrophy locus. *Cell*, **51**, 919–928.
3. Sicinski, P., Geng, Y., Ryder-Cook, A.S., Barnard, E.A., Darlison, M.G. and Barnard, P.J. (1989) The molecular basis of muscular dystrophy in the mdx mouse: a point mutation. *Science*, **244**, 1578–1580.
4. Gerhart, J., Bast, B., Neely, C., Iem, S., Amegbe, P., Niewenhuis, R., Miklasz, S., Cheng, P.F. and George-Weinstein, M. (2001) MyoD-positive myoblasts are present in mature fetal organs lacking skeletal muscle. *J. Cell Biol.*, **155**, 381–392.
5. Skuk, D., Goulet, M., Roy, B., Chapdelaine, P., Bouchard, J.P., Roy, R., Dugre, F.J., Sylvain, M., Lachance, J.G., Deschenes, L. *et al.* (2006) Dystrophin expression in muscles of Duchenne muscular dystrophy patients after high-density injections of normal myogenic cells. *J. Neuropathol. Exp. Neurol.*, **65**, 371–386.
6. Skuk, D., Goulet, M., Roy, B., Piette, V., Cote, C.H., Chapdelaine, P., Hogrel, J.Y., Paradis, M., Bouchard, J.P., Sylvain, M. *et al.* (2007) First test of a 'high-density injection' protocol for myogenic cell transplantation throughout large volumes of muscles in a Duchenne muscular dystrophy patient: eighteen months follow-up. *Neuromuscul. Disord.*, **17**, 38–46.
7. Dezawa, M., Ishikawa, H., Itokazu, Y., Yoshihara, T., Hoshino, M., Takeda, S., Ide, C. and Nabeshima, Y. (2005) Bone marrow stromal cells generate muscle cells and repair muscle degeneration. *Science*, **309**, 314–317.
8. De Bari, C., Dell'Accio, F., Vandenabeele, F., Vermeesch, J.R., Raymackers, J.M. and Luyten, F.P. (2003) Skeletal muscle repair by adult human mesenchymal stem cells from synovial membrane. *J. Cell Biol.*, **160**, 909–918.
9. Cui, C.H., Uyama, T., Miyado, K., Terai, M., Kyo, S., Kiyono, T. and Umezawa, A. (2007) Menstrual blood-derived cells confer human dystrophin expression in the murine model of Duchenne muscular dystrophy via cell fusion and myogenic transdifferentiation. *Mol. Biol. Cell*, **18**, 1586–1594.
10. Carosella, E.D., Paul, P., Moreau, P. and Rouas-Freiss, N. (2000) HLA-G and HLA-E: fundamental and pathophysiological aspects. *Immunol. Today*, **21**, 532–534.
11. Ulbrecht, M., Honka, T., Person, S., Johnson, J.P. and Weiss, E.H. (1992) The HLA-E gene encodes two differentially regulated transcripts and a cell surface protein. *J. Immunol.*, **149**, 2945–2953.
12. Braud, V.M., Allan, D.S., O'Callaghan, C.A., Soderstrom, K., D'Andrea, A., Ogg, G.S., Lazetic, S., Young, N.T., Bell, J.I., Phillips, J.H. *et al.* (1998) HLA-E binds to natural killer cell receptors CD94/NKG2A, B and C. *Nature*, **391**, 795–799.
13. Lee, N., Llano, M., Carretero, M., Ishitani, A., Navarro, F., Lopez-Botet, M. and Geraghty, D.E. (1998) HLA-E is a major ligand for the natural killer inhibitory receptor CD94/NKG2A. *Proc. Natl Acad. Sci. USA*, **95**, 5199–5204.
14. Borrego, F., Ulbrecht, M., Weiss, E.H., Coligan, J.E. and Brooks, A.G. (1998) Recognition of human histocompatibility leukocyte antigen (HLA)-E complexed with HLA class I signal sequence-derived peptides by CD94/NKG2 confers protection from natural killer cell-mediated lysis. *J. Exp. Med.*, **187**, 813–818.
15. Tsuji, H., Miyoshi, S., Ikegami, Y., Hida, N., Asada, H., Togashi, I., Suzuki, J., Satake, M., Nakamizo, H., Tanaka, M. *et al.* (2010) Xenografted human amniotic membrane-derived mesenchymal stem cells are immunologically tolerated and transdifferentiated into cardiomyocytes. *Circ. Res.*, **106**, 1613–1623.
16. Coupel, S., Moreau, A., Hamidou, M., Horejsi, V., Soulillou, J.P. and Charreau, B. (2007) Expression and release of soluble HLA-E is an immunoregulatory feature of endothelial cell activation. *Blood*, **109**, 2806–2814.
17. Faustman, D. and Coe, C. (1991) Prevention of xenograft rejection by masking donor HLA class I antigens. *Science*, **252**, 1700–1702.
18. Mendell, J.R., Kissel, J.T., Amato, A.A., King, W., Signore, L., Prior, T.W., Sahenk, Z., Benson, S., McAndrew, P.E., Rice, R. *et al.* (1995) Myoblast transfer in the treatment of Duchenne's muscular dystrophy. *N. Engl. J. Med.*, **333**, 832–838.
19. Mori, T., Kiyono, T., Imabayashi, H., Takeda, Y., Tsuchiya, K., Miyoshi, S., Makino, H., Matsumoto, K., Saito, H., Ogawa, S. *et al.* (2005) Combination of hTERT and bmi-1, E6, or E7 induces prolongation of the life span of bone marrow stromal cells from an elderly donor without affecting their neurogenic potential. *Mol. Cell. Biol.*, **25**, 5183–5195.
20. Li, J., Goldstein, I., Glickman-Nir, E., Jiang, H. and Chess, L. (2001) Induction of TCR Vbeta-specific CD8+ CTLs by TCR Vbeta-derived peptides bound to HLA-E. *J. Immunol.*, **167**, 3800–3808.
21. Hu, D., Ikizawa, K., Lu, L., Sanchirico, M.E., Shinohara, M.L. and Cantor, H. (2004) Analysis of regulatory CD8 T cells in Qa-1-deficient mice. *Nat. Immunol.*, **5**, 516–523.
22. Bryan, B.A., Walshe, T.E., Mitchell, D.C., Havumaki, J.S., Saint-Geniez, M., Maharaj, A.S., Maldonado, A.E. and D'Amore, P.A. (2008) Coordinated vascular endothelial growth factor expression and signaling during skeletal myogenic differentiation. *Mol. Biol. Cell*, **19**, 994–1006.
23. Darabi, R., Gehlbach, K., Bachoo, R.M., Kamath, S., Osawa, M., Kamm, K.E., Kyba, M. and Perlingeiro, R.C. (2008) Functional skeletal muscle regeneration from differentiating embryonic stem cells. *Nat. Med.*, **14**, 134–143.
24. Friedenstein, A.J., Gorskaja, J.F. and Kulagina, N.N. (1976) Fibroblast precursors in normal and irradiated mouse hematopoietic organs. *Exp. Hematol.*, **4**, 267–274.
25. Bieback, K., Kern, S., Kluter, H. and Eichler, H. (2004) Critical parameters for the isolation of mesenchymal stem cells from umbilical cord blood. *Stem Cells*, **22**, 625–634.
26. In 't Anker, P.S., Scherjon, S.A., Kleijburg-van der Keur, C., de Groot-Swings, G.M., Claas, F.H., Fibbe, W.E. and Kanhai, H.H. (2004) Isolation of mesenchymal stem cells of fetal or maternal origin from human placenta. *Stem Cells*, **22**, 1338–1345.
27. In 't Anker, P.S., Scherjon, S.A., Kleijburg-van der Keur, C., Noort, W.A., Claas, F.H., Willemze, R., Fibbe, W.E. and Kanhai, H.H. (2003) Amniotic fluid as a novel source of mesenchymal stem cells for therapeutic transplantation. *Blood*, **102**, 1548–1549.
28. Prockop, D.J. (1997) Marrow stromal cells as stem cells for nonhematopoietic tissues. *Science*, **276**, 71–74.
29. Kohyama, J., Abe, H., Shimazaki, T., Koizumi, A., Nakashima, K., Gojo, S., Taga, T., Okano, H., Hata, J. and Umezawa, A. (2001) Brain from bone: efficient 'meta-differentiation' of marrow stroma-derived mature osteoblasts to neurons with Noggin or a demethylating agent. *Differentiation*, **68**, 235–244.
30. Horwitz, E.M., Gordon, P.L., Koo, W.K., Marx, J.C., Neel, M.D., McNall, R.Y., Muul, L. and Hofmann, T. (2002) Isolated allogeneic bone marrow-derived mesenchymal cells engraft and stimulate growth in children with osteogenesis imperfecta: implications for cell therapy of bone. *Proc. Natl Acad. Sci. USA*, **99**, 8932–8937.
31. Miyoshi, H., Takahashi, M., Gage, F.H. and Verma, I.M. (1997) Stable and efficient gene transfer into the retina using an HIV-based lentiviral vector. *Proc. Natl Acad. Sci. USA*, **94**, 10319–10323.

Circulation Research
JOURNAL OF THE AMERICAN HEART ASSOCIATION

American Heart Association®
Learn and Live℠

Xenografted Human Amniotic Membrane Derived Mesenchymal Stem Cells Are Immunologically Tolerated and Transdifferentiated Into Cardiomyocytes

Hiroko Tsuji, Shunichiro Miyoshi, Yukinori Ikegami, Naoko Hida, Hironori Asada, Ikuko Togashi, Junshi Suzuki, Masaki Satake, Hikaru Nakamizo, Mamoru Tanaka, Taisuke Mori, Kaoru Segawa, Nobuhiro Nishiyama, Junko Inoue, Hatsune Makino, Kenji Miyado, Satoshi Ogawa, Yasunori Yoshimura and Akihiro Umezawa

Circ. Res. 2010;106;1613-1623
DOI: 10.1161/CIRCRESAHA.109.205260
Circulation Research is published by the American Heart Association. 7272 Greenville Avenue, Dallas, TX 72514
Copyright © 2010 American Heart Association. All rights reserved. Print ISSN: 0009-7330. Online ISSN: 1524-4571

The online version of this article, along with updated information and services, is located on the World Wide Web at:
http://circres.ahajournals.org/cgi/content/full/106/10/1613

Data Supplement (unedited) at:
http://circres.ahajournals.org/cgi/content/full/106/10/1613/DC1

Subscriptions: Information about subscribing to Circulation Research is online at
http://circres.ahajournals.org/subscriptions/

Permissions: Permissions & Rights Desk, Lippincott Williams & Wilkins, a division of Wolters Kluwer Health, 351 West Camden Street, Baltimore, MD 21202-2436. Phone: 410-528-4050. Fax: 410-528-8550. E-mail:
journalpermissions@lww.com

Reprints: Information about reprints can be found online at
http://www.lww.com/reprints

Downloaded from circres.ahajournals.org at KEIO UNIV IGAKUBU LIB on March 15, 2011

Xenografted Human Amniotic Membrane–Derived Mesenchymal Stem Cells Are Immunologically Tolerated and Transdifferentiated Into Cardiomyocytes

Hiroko Tsuji,* Shunichiro Miyoshi, Yukinori Ikegami,* Naoko Hida, Hironori Asada, Ikuko Togashi, Junshi Suzuki, Masaki Satake, Hikaru Nakamizo, Mamoru Tanaka, Taisuke Mori, Kaoru Segawa, Nobuhiro Nishiyama, Junko Inoue, Hatsune Makino, Kenji Miyado, Satoshi Ogawa, Yasunori Yoshimura, Akihiro Umezawa

Rationale: **Amniotic membrane is known to have the ability to transdifferentiate into multiple organs and is expected to stimulate a reduced immunologic reaction.**

Objective: **Determine whether human amniotic membrane–derived mesenchymal cells (hAMCs) can be an ideal allograftable stem cell source for cardiac regenerative medicine.**

Methods and Results: **We established hAMCs. After cardiomyogenic induction in vitro, hAMCs beat spontaneously, and the calculated cardiomyogenic transdifferentiation efficiency was 33%. Transplantation of hAMCs 2 weeks after myocardial infarction improved impaired left ventricular fractional shortening measured by echocardiogram (34±2% [n=8] to 39±2% [n=11]; $P<0.05$) and decreased myocardial fibrosis area (18±1% [n=9] to 13±1% [n=10]; $P<0.05$), significantly. Furthermore hAMCs transplanted into the infarcted myocardium of Wistar rats were transdifferentiated into cardiomyocytes in situ and survived for more than 4 weeks after the transplantation without using any immunosuppressant. Immunologic tolerance was caused by the hAMC-derived HLA-G expression, lack of MHC expression of hAMCs, and activation of FOXP3-positive regulatory T cells. Administration of IL-10 or progesterone, which is known to play an important role in feto-maternal tolerance during pregnancy, markedly increased HLA-G expression in hAMCs in vitro and, surprisingly, also increased cardiomyogenic transdifferentiation efficiency in vitro and in vivo.**

Conclusions: **Because hAMCs have a high ability to transdifferentiate into cardiomyocytes and to acquire immunologic tolerance in vivo, they can be a promising cellular source for allograftable stem cells for cardiac regenerative medicine.** (*Circ Res.* **2010;106:1613-1623.**)

Key Words: cardiomyogenesis ■ human mesenchymal stem cell ■ immunologic tolerance ■ myocardial infarction ■ cell-based therapy

Although embryonic stem cells[1] and induced pluripotent stem (iPS) cells[2] can be differentiated into cells of various organs, including cardiomyocytes, there are many underlining problems to overcome before clinical applications can be used, eg, tumorigenicity.[3] Autografts of iPS cells may not cause immunologic rejection; ironically, however, possible neoplasm formation would cause a serious problem because the neoplasm would not be rejected by the withdrawal of immunosuppressive agents. On the other hand, mesenchymal stem cells (MSCs) have recently been used for clinical application, and their safety and feasibility in cardiac stem cell-based therapy have been demonstrated.[4] Thus, MSCs are a more important cellular source for stem cell-based therapy from a practical point of view.

The efficacy of human bone marrow–derived MSCs (BMMSCs) was still limited,[5] however, because of low efficiency for cardiomyogenic transdifferentiation.[6] We previously reported that non–marrow-derived mesenchymal cells had higher cardiomyogenic transdifferentiation efficiency, eg, menstrual blood–derived mesenchymal cells (MMCs),[7] umbilical cord blood–derived mesenchymal stem cells (UCB-MSCs),[8] and placental chorionic plate–derived mesenchymal cells (PCPCs).[9] These cells are thought to be used by an allograft; therefore, problems of immunologic rejection arise. However, an allograft may be superior to an autograft in several ways. Taking into account the background condition of the patient (eg, metabolic disease or age),

Original received July 16, 2009; revision received April 14, 2010; accepted April 22, 2010.

From the Departments of Obstetrics (H.T., H.A., M.T., Y.Y.), Cardiology (S.M.,Y.I., N.H., I.T., J.S., M.S., H.N., N.N., S.O.), Pathology (T.M.), and Microbiology and Immunology (K.S.) and Institute for Advanced Cardiac Therapeutics (S.M.), Keio University School of Medicine; and Department of Reproductive Biology and Pathology (H.T., Y.I., N.H., N.N., H.M., K.M., A.U.), National Research Institute for Child Health and Development. J.I. is a freelance translator.

*Both authors contributed equally to this work.

Correspondence to Shunichiro Miyoshi, MD, PhD, Keio University School of Medicine, 35-Shinanomachi, Shinjuku-ku, Tokyo, 160-8582, Japan. E-mail smiyoshi@cpnet.med.keio.ac.jp

© 2010 American Heart Association, Inc.

Circulation Research **is available at http://circres.ahajournals.org** **DOI: 10.1161/CIRCRESAHA.109.205260**

Downloaded from circres.ahajournals.org at KEIO UNIV IGAKUBU LIB on March 15, 2011

Non-standard Abbreviations and Acronyms	
AP	action potential
BMMSC	bone marrow–derived mesenchymal stem cell
EGFP	enhanced green fluorescent protein
FISH	fluorescent in situ hybridization
IL	interleukin
hAMC	human amniotic membrane–derived mesenchymal stem cell
hANP	human atrial natriuretic peptide
HLA	human leukocyte antigen
iPS	induced pluripotent stem
MHC	major histocompatibility complex
MI	myocardial infarction
MMC	menstrual blood–derived mesenchymal cell
MSC	mesenchymal stem cell
PCPC	placental chorionic plate–derived mesenchymal stem cell
PD	population doubling
UCB-MSC	umbilical cord blood–derived mesenchymal cell

stem cells obtained from young and healthy volunteers are expected to have a better efficacy in stem cell therapy.[10,11] Previously, mesenchymal cells did not express HLA-DR[6–9,12] and are believed to resist immunologic rejection to some extent. Shake et al[13] showed that xenografted mesenchymal cells were immunologically tolerated in the host heart. These cells, however, failed to show clear cardiomyogenic differentiation, and the mechanisms of tolerance were not well investigated. Unlike other mesenchymal cells (BMMSC, MMC, UCB-MSC, PCPC), only human amniotic membrane–derived mesenchymal stem cells (hAMCs) do not express the major histocompatibility complex (MHC) class I molecule and may be expected to show immunologic tolerance.

Recently, amniotic membrane–derived cells were reported to have potential for transdifferentiation into cells of various organs. Zhao et al,[14] and Miki et al,[15] reported evidence of possible cardiomyogenic transdifferentiation ability, but failed to show functioning cardiomyocytes. Fujimoto et al,[16] reported significant recovery of cardiac function by the rat amnion-derived cell transplantation in rat myocardial infarction (MI) model, however, they failed to show clear evidence of cardiomyogenic differentiation in vivo. Therefore, in the present study, we attempted to show: (1) the powerful cardiomyogenic transdifferentiation potential of our isolated hAMCs, and the beneficial effect of transplantation of hAMCs on cardiac function in vivo; (2) the induction of immunologic tolerance so that hAMCs can be a powerful allograftable stem cell source without either the administration of immunosuppressive agents or matching of MHC typing; (3) the mechanism of induction of tolerance; and (4) the close relationship between the cardiomyogenic transdifferentiation of mesenchymal cells and the process of immunologic tolerance.

Methods

An expanded Methods section is available in the Online Data Supplement at http://circres.ahajournals.org.

Isolation and Culture of Human Amniotic Membrane–Derived Mesenchymal Cells

Human amniotic membrane was collected, with informed consent from individual patients, after delivery of a male neonate. The study was approved by the ethics committee of Keio University School of Medicine. The precise methods for culture have been described previously.[9,17] Detail is shown in the Online Data Supplement.

Coculture With Murine Fetal Cardiomyocytes

Cardiomyocytes were obtained from hearts of day-17 mouse fetuses.[6–9] The isolated cardiomyocytes were replated at $5\times10^4/cm^2$ on top of a floating atelocollagen film,[7,8] or on the bottom of a culture dish. The human amniotic membrane–derived mesenchymal cell (hAMCs) were infected with enhanced green fluorescent protein (EGFP)-expressing adenovirus.[6–9] The hAMCs were harvested and seeded on top of the cardiomyocytes (Figure 1H and 1I; Figure 2A, 2B, and 2H through 2M; Figure 3; Online Figure III) or on the bottom of the atelocollagen film (Figure 2D through 2F; Online Figure III) at $3\times10^3/cm^2$. For blocking experiments, neutralizing antibodies directed to HLA-G (clone 87G; Exbio) and IL10 (ab22771; Abacam) were added at a concentration of 20 μg/mL every day from 1 day before coculture till day 7. To prove the effect of immunologic reaction to the coculture system, we used the following immunosuppressive agents from one day before the coculture to day 7: FK506 (tacrolimus, 20 ng/mL, F4679, Sigma-Aldrich) and hydrocortisone (1 μg/mL, H0396, Sigma-Aldrich). In some experiment we used EGFP transgenic mouse fetuses (C57BL/6[18]).

Immunocytochemistry and Immunohistochemistry

A laser confocal microscope (FV1000, Olympus) was used for immunocytochemical analysis. Samples were stained with anti–cardiac troponin-I antibody or anti–sarcomeric α-actinin antibody and anti–connexin 43 antibody, as described previously.[7–9] In the present study, we used anti-FOXP3 antibody (IMGENEX, IMG-5276A), anti–HLA-G antibody (Abcam, ab7758), and anti-hANP antibody (YLEM, MCV928) according to the manufacturer's recommendation. The cells were isolated and stained immunocytochemically, and then observed by confocal laser microscope. The cardiomyogenic transdifferentiation efficiency was calculated as the fraction of cardiac troponin-I positive cells in the EGFP-positive cells.[7–9] Detail is shown in the Online Data Supplement. The methods to evaluate in vitro transdifferentiation potential to the noncardiac organs are provided in the Online Data Supplement.

Reverse Transcriptase–Polymerase Chain Reaction

RT-PCR was done as described previously.[6–9] PCR primers were prepared such that they would amplify the human but not the mouse genes. Primers for cardiomyocyte-related genes were used (see also Online Table I).

Western Blot and ELISA

Western blot analysis for hAMCs was done by iBlot dry blotting system (Invitrogen) according to the manufacturer's recommendation. Proteins were extracted from 1×10^6 hAMCs, placenta-derived mesenchymal cells, and menstrual blood–derived mesenchymal cells. Cellular lysates were electroblotted and probed using the anti–HLA-G IgG monoclonal antibody (1 μg/mL; EXBIO). Collected images were analyzed by the Image J software (http://rsbweb.nih.gov/ij/). The calculated data were normalized by the data of b-actin. Soluble HLA-G was measured by enzyme-linked immunosorbent assay (ELISA) in plates coated with the captured antibody MEM-G/09 (sHLA-G Kit; Exbio, Czech Republic), according to the manufacturer's recommendation. JEG3 (GeneTex, GTX14841) was used for the positive control of HLA-G.

Fluorescent In Situ Hybridization

The CEP X/Y DNA Probe Kit (Vysis) was used to determine the proportion of XX and XY cells according to the manufacturer's recommendation.[9] The Alu probe (BIOGENEX, PR-100101) was used according to the manufacturer's recommendation.

Downloaded from circres.ahajournals.org at KEIO UNIV IGAKUBU LIB on March 15, 2011

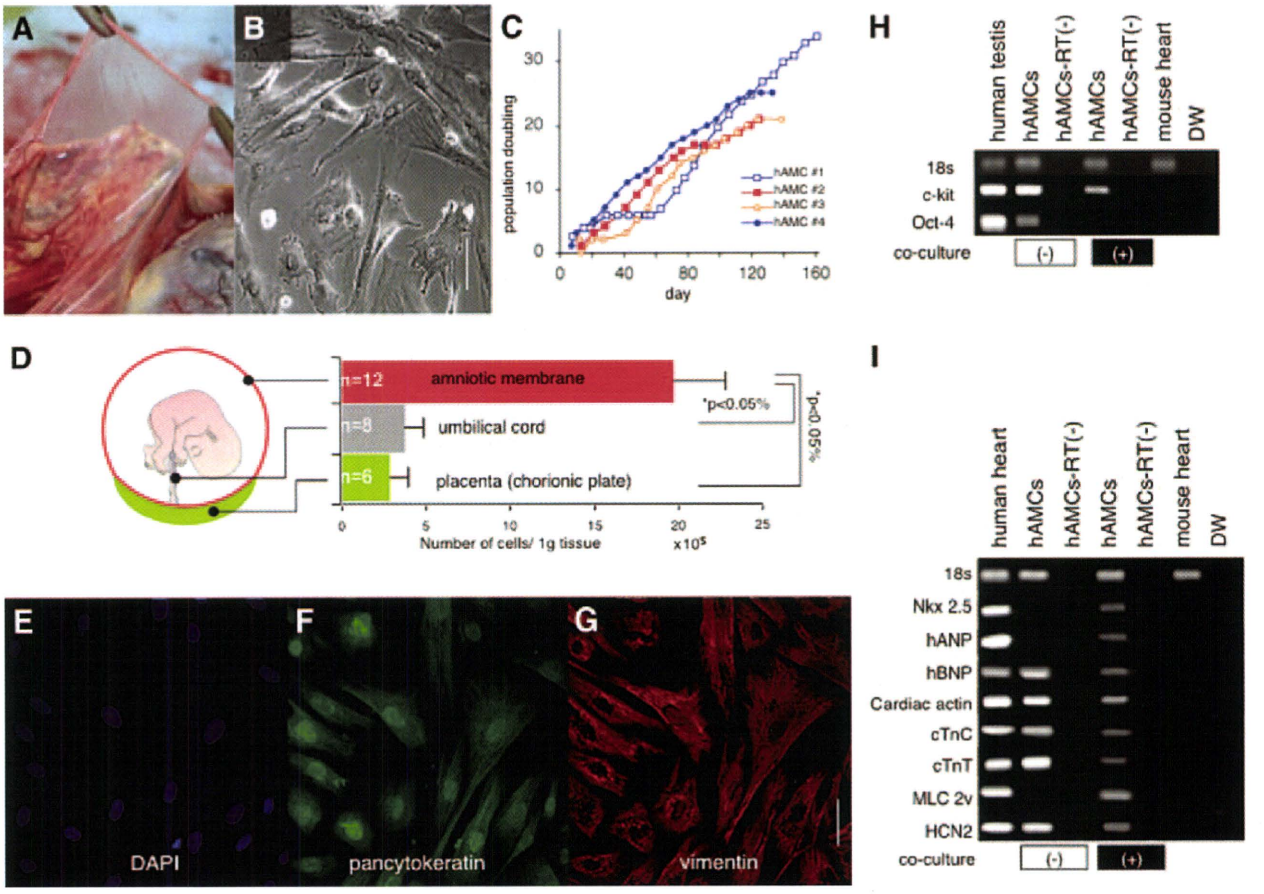

Figure 1. Cellular phenotype, surface marker, and expression of cardiomyocyte-specific genes. A, Macroscopic view of amniotic membrane. **B,** Phase contrast microscopic view of hAMCs. **C,** The representative growth curves of hAMCs as a function of time after the culture. **D,** Numbers of collected mesenchymal cells obtained from 1 g of placental tissues at 2 weeks after the start of culture are shown. n indicates number of delivery. **E through G,** Laser confocal microscopic view of immunocytochemistry of hAMCs in culture with anti-pancytokeratin **(green; F)** and anti-vimentin **(red; G)** antibodies. **H and I,** RT-PCR was performed with PCR primers with specificity for human genes encoding cardiac proteins but not for the corresponding murine genes (Online Table I) before (−, **white box**) and after (+, **black box**) the coculture. **H,** RT-PCR for stem cell markers was performed. hAMCs express Oct-4 and c-kit at the default state. **I,** Human heart cells and mouse heart cells were used as a positive control and negative control, respectively. Most human cardiac genes were expressed after the coculture. **Scale bars:** 20 μm **(B and G).**

Physiological Analysis

Functional analysis was performed at 1 week after the cardiomyogenic induction. The method of action potential (AP) recording was as previously described.[6–9] Alexa 568 was injected into cells via recording microelectrodes to stain the cells and confirm that the AP was generated by EGFP-positive cells (Figure 1B). Contraction of the cells was measured by the video image of EGFP-positive cells as described previously.[7–9]

hAMC Transplantation in Myocardial Infarction Model In Vivo

Myocardial infarction (MI) was induced in the open chests of anesthetized Wistar rats (8 weeks of age) or of F344 nude rats (Clea Japan Inc) (6 weeks of age), as described previously.[7,19] Two weeks after the MI, 1 to 2×10^6 of EGFP-labeled hAMCs were injected into the myocardium at the border zone of the MI[7]; they survived without using an immunosuppressive agent. In some experiment EGFP-transgenic mouse[18] was uses as recipients. To examine the effect of hAMC transplantation in vivo, we selected nude rats as recipients.[7] Two weeks after the first operation, nude rats with MI were randomized in a blind study of the following groups: the control MI group (MI), the MI+hAMC transplanted group (MI+hAMC), and the sham operated group (sham). Randomization occurred immediately before echocardiogram. Immediately before cell transplantation, 2D and M-mode echocardiographic (8.5-MHz linear transducer; EnVisor C, Phillips Medical System, Andover, Mass) images were obtained to assess left ventricular end-diastolic dimension and left ventricular end-systolic dimension at the midpapillary muscle level. Two weeks after the transplantation, a similar echocardiogram was performed again. ECG and left ventricular pressure were measured as previously described.[7] Tissue samples were obtained by slicing along the short axis of the left ventricle, for every 1 mm of depth. After Masson's trichrome staining, the area of fibrosis was digitized from each slice, and then the percentage of fibrosis area in the left ventricular myocardium was calculated, as previously described.[7] To test the potential induction of immunologic tolerance, hAMCs were transplanted into the Wistar rats. Hearts and sera were obtained at between 2 days to 56 days after hAMC transplantation, and then analyzed by immunohistochemistry, fluorescent in situ hybridization (FISH), and ELISA experimental methodologies. The survival rate of EGFP-positive cardiomyocytes was calculated by fluorescent microscope (details are shown in the Online Data Supplement). In some experiments, hAMCs were pretreated with 10 ng/mL of IL10 (Sigma I9276) or 10 ng/mL of progesterone (p7556; Sigma-Aldrich) for 2-days before the transplantation to observe the efficacy of survival of hAMCs in vivo. Enzymatically isolated EGFP-positive cardiomyocytes[20,21] were selected by glass pipette driven by a manipulator mounted on the inverted fluorescent microscope, then used for the FISH experiment to determine the origin of EGFP-positive transdifferentiated cardiomyocytes. See also the Online Data Supplement.

Downloaded from circres.ahajournals.org at KEIO UNIV IGAKUBU LIB on March 15, 2011

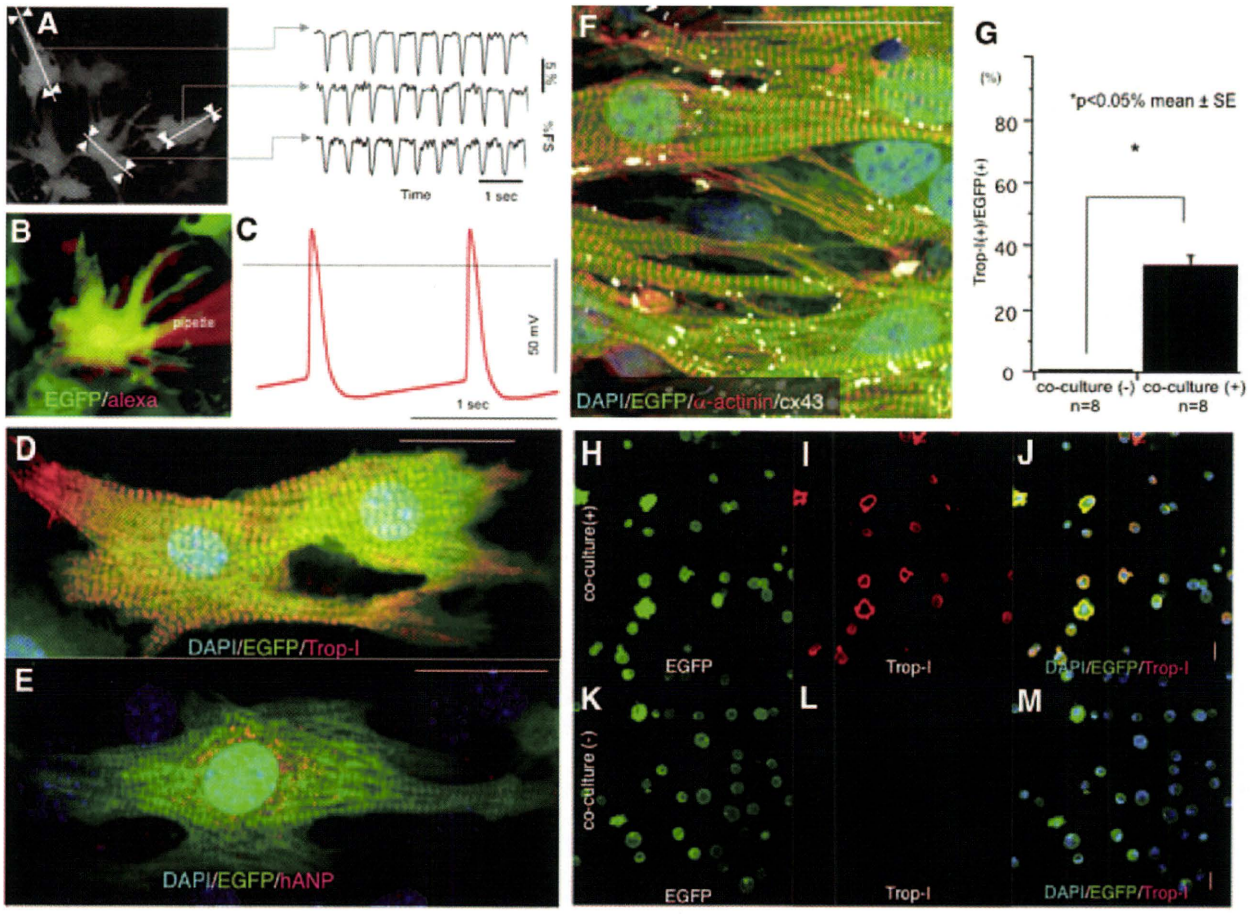

Figure 2. Cardiomyogenic differentiation of hAMCs in vitro. A, Still image **(left)** and detected fractional shortening (%FS), along the **white lines** between the **white arrows**, are shown in the **right panel**. **B,** EGFP-labeled hAMCs were injected with Alexa 568 solution **(red)** through microelectrodes to confirm that the recorded signal was obtained from hAMCs. **C,** Representative AP traces are shown (horizontal line denotes 1 second). The vertical line denotes 50 mV and the dotted horizontal line denotes 0 mV. **D through F,** Laser confocal microscopic view of immunocytochemistry of differentiated hAMCs with anti–cardiac troponin I (Trop-I) **(D)**, anti-human atrial natriuretic peptide (hANP) **(E)**, anti–sarcomeric α-actinin (α-actinin) **(F)** (see also Online Figure III), and anti–connexin 43 (Cx43) **(F)** antibodies. EGFP-positive **(green)** hAMCs expressed troponin I **(red)**, hANP **(red)**, α-actinin **(red)**, and Cx-43 **(white)**. Nuclei were stained with DAPI **(blue)**. **Scale bar:** 20 μm. Clear striation pattern of troponin I and α-actinin, and diffuse dot-like staining of connexin 43 and hANP were observed. **G,** Cardiomyogenic transdifferentiation efficiency before (−) and after (+) the coculture of hAMCs. **H through M,** Representative immunocytochemical images of troponin I for enzymatically isolated differentiated hAMCs with and without coculture. **Scale bar:** 20 μm.

Statistical Analysis

All data are shown as the mean value ± SE. The difference between two mean values was determined with a Student *t* test. The difference among more than 3 mean values was determined with one-way ANOVA test or one-way repeated measures ANOVA test and Bonferroni post hoc test. Statistical significance was set at $P<0.05$.

Results

This study was approved by the institutional ethical committee. With informed consent, human placenta and amniotic membrane were collected after delivery of a male neonate. The amniotic membrane was pealed off from the maternal placenta (Figure 1A) and hAMCs (Figure 1B) were collected by the culture method, as described previously.[9,17] The hAMCs proliferated at 18 to 22 population doublings (PDs) (Figure 1C), and experiments were performed on hAMCs at 2 to 9 PDs unless otherwise mentioned. The number of mesenchymal cells at 3 days after the primary culture per 1g tissue samples from the amniotic membrane, umbilical cord, and placenta[9] are shown in Figure 1D. This suggests that the amniotic membrane is a rich cellular source of mesenchymal cells. FISH analysis for human chromosome X and Y revealed that 100% of the obtained cells were of male infant origin. Immunocytochemical analysis revealed that hAMCs expressed both pancytokeratin and vimentin, suggesting hAMCs have both epithelial and mesenchymal phenotypes (Figure 1E through EG). Surface marker analysis (Online Figure I) revealed that hAMCs did not express hematopoietic linage markers, eg, CD14, CD34, CD45, CD117, and CD309, and did express mesenchymal linage markers, eg, CD10, CD29, CD44, and CD105. It is noteworthy that hAMCs were positive for SSEA4,[22] an embryonic stem cell marker. hAMCs were negative for HLA-ABC, HLA-D, and HLA-DR. The RT-PCR was performed with primers that hybridized with human-specific genes but not with the murine orthologs.[6–8] The hAMCs expressed Oct-4 and c-kit (Figure 1H) and did not express Nkx2.5 before cardiomyogenic induction (Figure 1I). Almost all cardiac-specific genes were expressed after cardiomyogenic induction (Figure 1I).

Downloaded from circres.ahajournals.org at KEIO UNIV IGAKUBU LIB on March 15, 2011

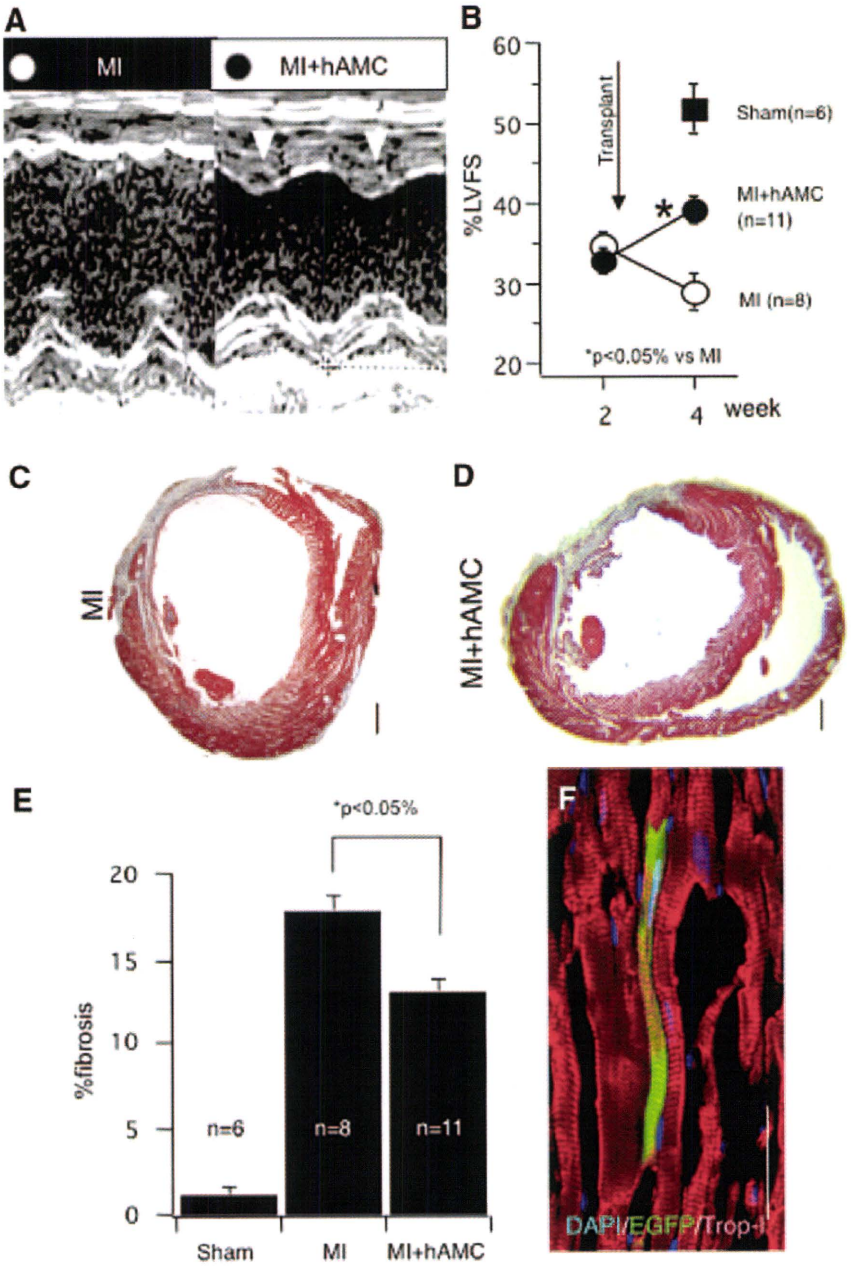

Figure 3. Effect of hAMC transplantation on heart function in vivo. A, Representative traces of M-mode echocardiogram from the control MI of nude rats and MI+hAMC transplanted nude rats (MI+hAMC) are shown. The contraction of the left ventricular anterior wall was improved by transplantation of hAMCs **(white arrows). B,** The hAMC transplantation significantly increased in measured percentage of left ventricular fractional shortening (%LVEF) at 4 weeks after the first operation. **C and D,** Representative Masson's trichrome staining of the heart at the papillary muscle level is shown. The digitized data were measured and calculated in **E**. The hAMC transplantation significantly decreased in percentage of fibrosis area. **Scale bar:** 1 mm. **F,** Merged image of confocal laser microscopic view of immunohistochemistry with anti–cardiac troponin I antibody (Trop-I) **(red)**, DAPI **(blue)**, and EGFP **(green)**. The EGFP-positive hAMC-derived cardiomyocytes were observed at the margin of the MI area of the nude rats. **Scale bar:** 50 μm.

Cardiomyogenic induction of hAMCs was performed by a coculture system with fetal murine cardiomyocytes, as described previously.[6–9] EGFP-labeled hAMCs started beating within a few days after the induction and about half of the hAMCs spontaneously contracted in a synchronized manner (Figure 2A); the averaged percentage of fractional shortening (%FS) was 6.2±0.6% (n=8). The recorded AP from EGFP-positive hAMCs (Figure 2B) showed pacemaker-like potential (n=7) and cardiomyocyte-specific long AP duration (Figure 2C). Averaged amplitude was 71.5±2.2 mV, maximal diastolic potential was -52.7±1.9 mV, AP duration at 90% repolarization was 161.6±9.3 ms, and beating cycle length was 1.06±0.1 s (n=7). Cardiomyogenic transdifferentiation could be observed when the murine cardiomyocytes and hAMCs were separately cocultured by the atelocollagen membrane (Figure 2D through 2F; Online Figure III) that is permeable for only small molecules (less than 5,000MW).[7,8] In another experiment murine cardiomyocytes were stained with MitoTracker Red (Invitrogen, M7512) and cocultured with hAMCs, then we confirmed that almost all EGFP positive cardiomyocytes were MitoTracker negative (Online Figure II, A through E). On the other hand hAMCs were stained with the MitoTracker Red and cocultured with EGFP-transgenic murine cardiomyocytes, then we confirmed that almost all MitoTracker positive cardiomyocytes were EGFP negative (Online Figure II, F through J). Thus, we concluded that the observed EGFP-positive cardiomyocytes were caused not by cell fusion between murine cardiomyocytes and hAMCs, but by transdifferentiation of hAMCs. Immunocytochemical analysis revealed a clear striation pattern of cardiac troponin-I (Figure 2D), dot-like pattern of human atrial natriuretic peptide (hANP) (Figure 2E), clear striation

Downloaded from circres.ahajournals.org at KEIO UNIV IGAKUBU LIB on March 15, 2011

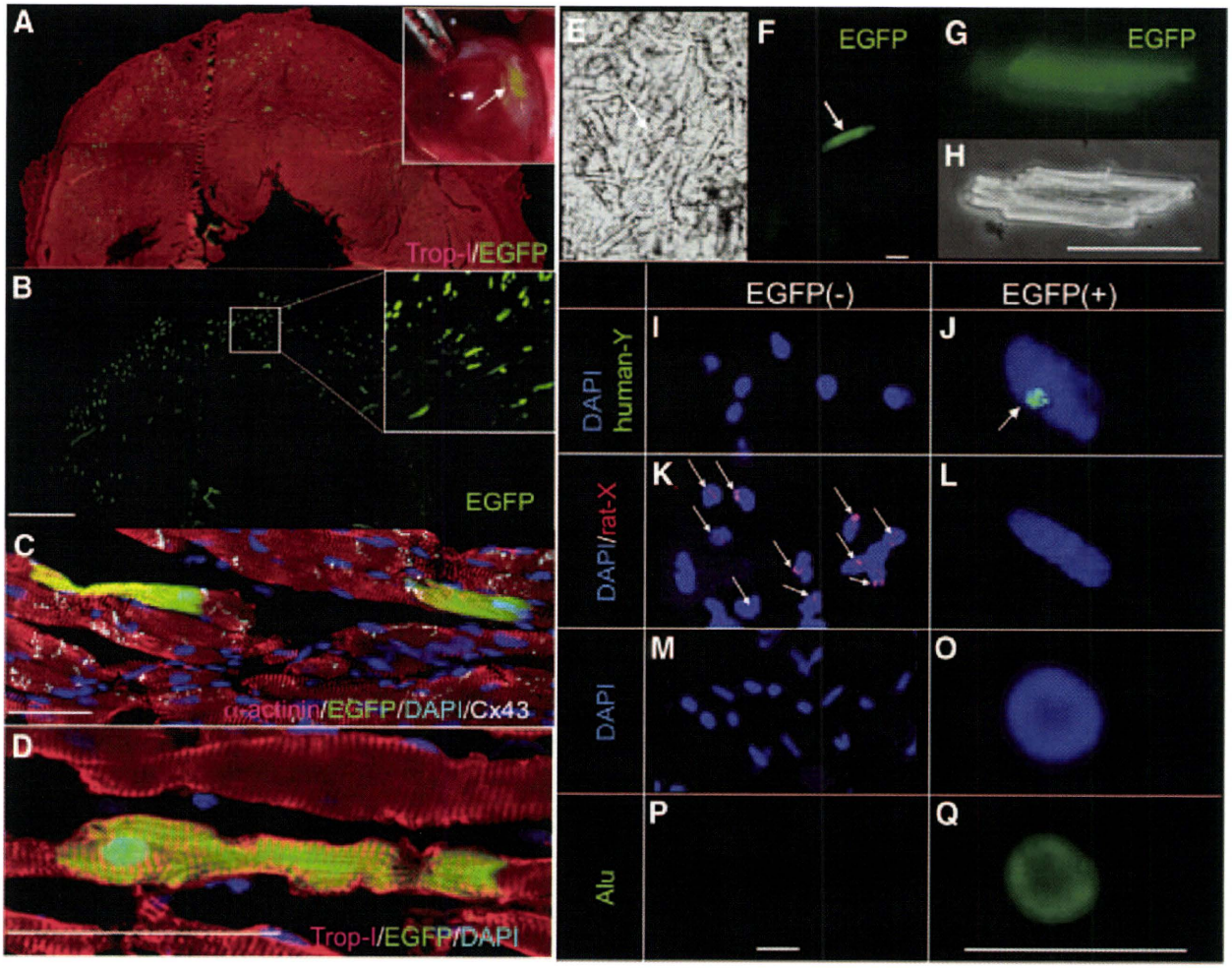

Figure 4. Survival of xenografted hAMCs transdifferentiated into cardiomyocytes in vivo. EGFP-labeled hAMCs were transplanted into the myocardium at the margin of MI of Wistar rat hearts (**white arrow** in the inset of **A**) and survived for 2 weeks. **A and B,** Fluorescent microscopic view of immunohistochemistry of left ventricle at 2 weeks after the transplantation with anti–cardiac troponin-I (Trop-I) **(red) (B)** EGFP **(green)** and **(A)** merged image with EGFP and troponin I. Significant numbers of EGFP-positive cells were observed at the margin of MI by lower magnification view **(B)** (see also Online Figure VI; Figure VII, F through J). **C and D,** Laser confocal microscopic view of immunohistochemistry of differentiated EGFP-positive hAMCs (4 weeks after transplantation) with anti–sarcomeric α-actinin (α-actinin) **(red; C)**, anti–connexin 43 (Cx43) **(white; C)**, and anti–troponin I **(red; D)** antibodies (see also Online Figure VII, A through E). **E through H,** Phase contrast image **(E and H)** and fluorescent image **(F and G)** in the same visual field of cardiomyocytes immediately after enzymatic isolation **(E and F)** and after selection of EGFP-positive cardiomyocytes **(G and H). I through Q,** FISH analysis for human Y chromosome **(green; I and J)**, rat X chromosome **(red; K and L)**, and human-specific Alu **(green; P and Q)** of EGFP-negative **(I, K, M, and P)** and EGFP-positive **(J, L, O, and Q)** cardiomyocytes. Nuclei staining by DAPI **(blue)** in the same visual filed of **P and Q** are shown in **M and O**, respectively. EGFP-positive cardiomyocytes were of human origin. **Scale bars:** 1 mm **(B)**; and 50 μm **(C, D, F, and H)**; 20 μm **(P and Q)**.

pattern of α-actinin, and dotted staining of connexin 43 (Figure 2F and Online Figure III). The percentage of cardiac troponin-I positive cells in the EGFP-positive cells was defined by immunocytochemical analysis (Figure 2G through 2M) and calculated to determine the cardiomyogenic transdifferentiation efficiency.[7–9] The efficiency was significantly increased up to 33±3% (n=8) by the cocultivation.

The hAMCs were transplanted into the hearts of nude rats with chronic MI, in vivo, and the effect on cardiac function was examined. Echocardiography showed a significant increase in the left ventricular fractional shortening (%LVFS) at 2 weeks after transplantation (Figure 3A and 3B; see also Online Figure IV). The heart section was stained with Masson's trichrome (Figure 3C and 3D) and the MI area was digitized and measured (Figure 3E). The percentage of fibrosis area was significantly decreased by hAMC transplantation (MI n=8, MI+hAMC n=11, $P<0.05$). The EGFP-positive cells of hAMCs (Figure 3F) observed at the MI area expressed a clear striation staining pattern of cardiac troponin-I, suggesting in situ cardiomyogenic transdifferentiation ability for hAMCs. The rate of survived EGFP-positive cardiomyocytes was 1.125±0.470% (n=6).

We tested whether xenografted hAMCs may be immunologically tolerated to survive for more than 2 weeks and differentiate into cardiomyocytes in situ. Isolated hAMCs were injected into the MI zone of female Wistar rats (Figure 4A, inset, white arrow). A significant number of EGFP-labeled rod-shaped cardiomyocytes were observed (Figure 4A and 4B), even 2 weeks after the transplantation (at least 80 days; Online Figure V). Immunohistochemistry revealed that

Downloaded from circres.ahajournals.org at KEIO UNIV IGAKUBU LIB on March 15, 2011

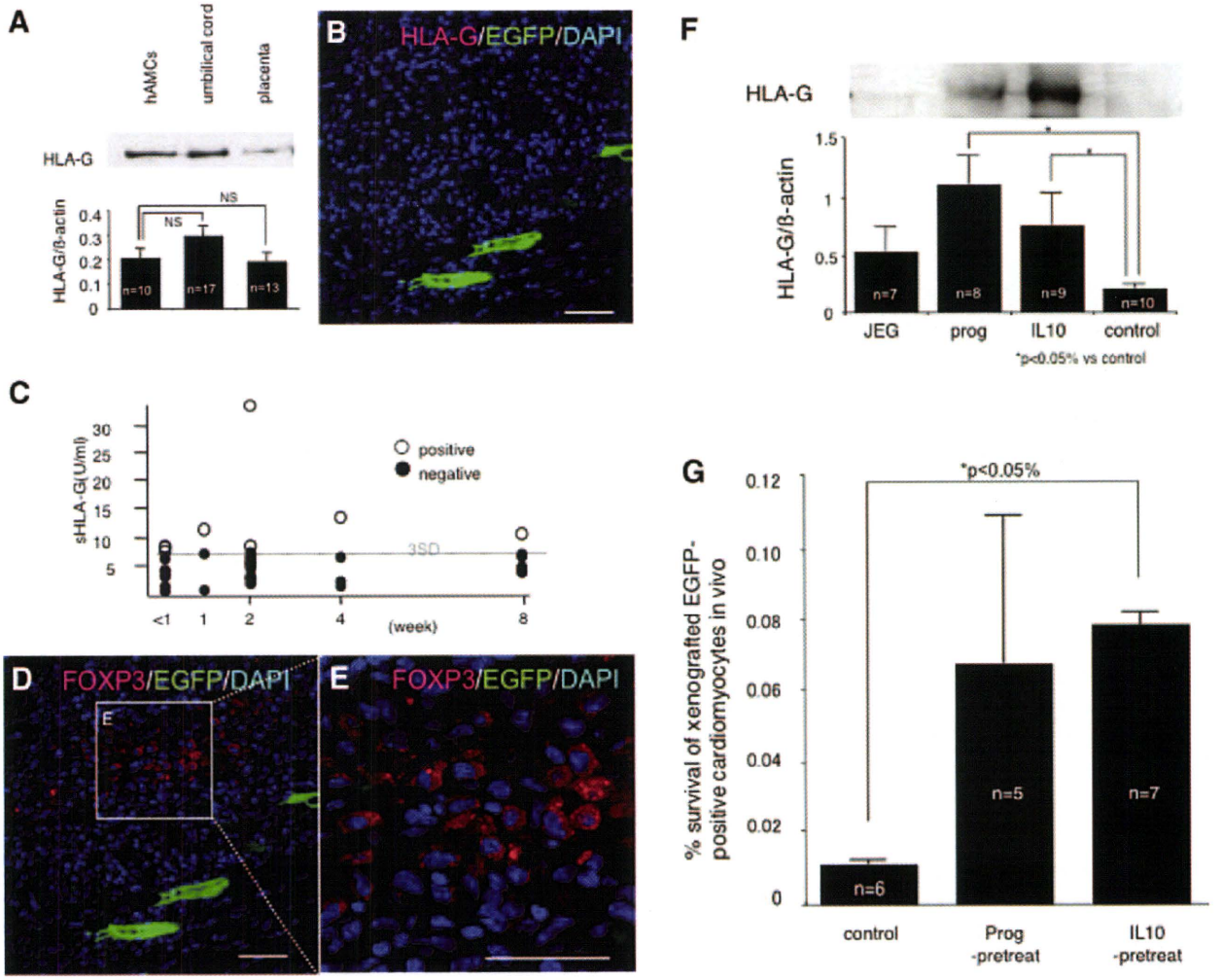

Figure 5. Role of HLA-G and regulatory T cells in immunologic tolerance of xenografted hAMCs. A, Western blot analysis of HLA-G in the mesenchymal cells obtained from amniotic membrane (hAMCs), umbilical cord, and placenta. Densitometry analysis of HLA-G, normalized by β-actin. **B,** Laser confocal microscopic view of immunohistochemistry of host myocardium (2 weeks after transplantation) with anti–HLA-G antibody **(red)**. The transdifferentiated EGFP-positive cardiomyocytes did not show any membrane biding isoform of HLA-G in situ. **C,** Concentration of the soluble form of HLA-G (sHLA-G) in the sera of hAMC transplanted Wistar rats detected by ELISA as a function of time in weeks after the transplantation is shown. There is no correlation between the survival of EGFP-positive cardiomyocytes and sHLA-G concentration. **D,** Immunohistochemistry with anti-FOXP3 **(red)** antibody. **E,** Expansion of **area within the white box** in **D** (see also Online Figure IX). A significant number of FOXP3-positive regulatory T cells have migrated beside the hAMC-derived cardiomyocytes. **F,** The effect of agents related to fetomaternal immunologic interaction on the HLA-G expression in the hAMCs was tested by Western blot analysis. Densitometric data were normalized by b-actin. Both IL10 and progesterone (prog) markedly increased the HLA-G expression in hAMCs. Concordant with **F**, pretreatment with progesterone and IL10 significantly increased the survival rate of xenografted hAMC-derived cardiomyocytes in the Wistar rat heart **(G). Scale bars:** 50 μm **(B,D, and E)**.

they were positive for sarcomeric α-actinin, connexin 43, and cardiac troponin-I (Figure 4C and 4D; Online Figures VI and VII). Host hearts were enzymatically isolated (Figure 4E and 4F), then EGFP-positive cardiomyocytes were selected (Figure 4G and 4H). FISH analysis to detect the human-Y and the rat-X chromosome revealed that the EGFP-negative cardiomyocytes express the rat-X chromosome and no human-Y chromosome (Figure 4I and 4K), whereas the EGFP-positive cardiomyocytes express the human-Y chromosome and no rat-X chromosome (Figure 4J and 4L). FISH analysis to detect Alu,[23] which is a human-specific short interspersed repetitive element, revealed that the EGFP-negative cardiomyocytes were negative for Alu (Figure 4M and 4P), whereas the EGFP-positive cardiomyocytes were positive for Alu (Figure 4O and 4Q). From these findings, we concluded that neither cell fusion nor nuclear fusion was the major cause of generation of EGFP-positive cardiomyocytes, but that the hAMCs transdifferentiated into cardiomyocytes and were immunologically tolerated, surviving more than 80 days in situ. In some experiment non–EGFP-labeled hAMCs was transplanted into the MI zone of EGFP-transgenic mouse, and observed EGFP-negative sarcomeric α-actinin positive hAMCs derived cardiomyocytes was observed (Online Figure VIII).

Before the transplantation, HLA-G was consistently detected in hAMCs by western blot analysis, and was also detected in mesenchymal cells obtained from other placenta-related organs (Figure 5A). After transplantation, however, HLA-G was detected only inconsistently in situ. No membrane-binding isoform of HLA-G was detected in the surviving hAMC-derived cardiomyocytes in Wistar rat hearts

Downloaded from circres.ahajournals.org at KEIO UNIV IGAKUBU LIB on March 15, 2011

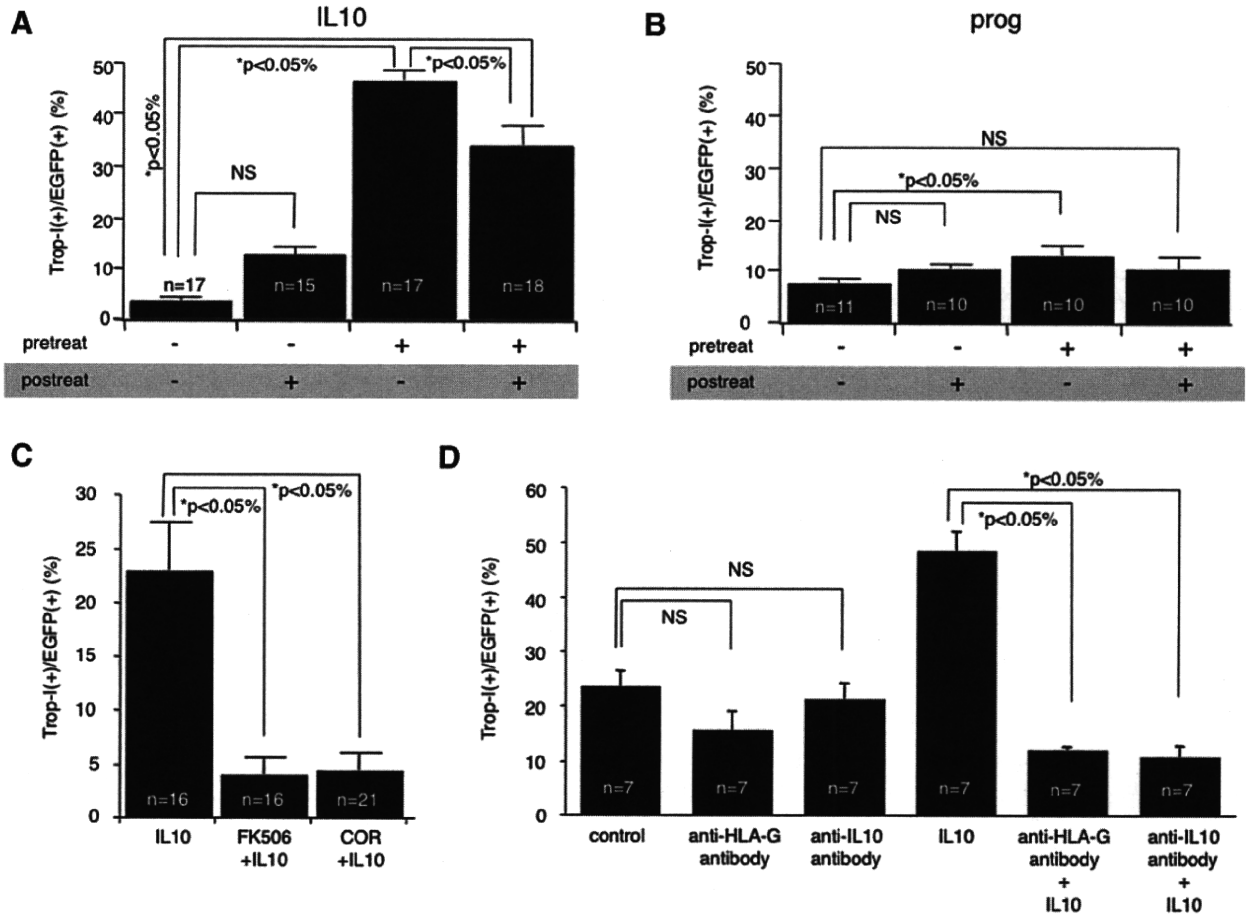

Figure 6. The effect of IL10, progesterone, and immunosuppressive agents on cardiomyogenic transdifferentiation efficiency of hAMCs. The effect of IL10 **(A)** and progesterone (prog) **(B)** on the cardiomyogenic transdifferentiation efficiency was measured. These agents were administered 2 days before the cocultivation (pretreat) and/or after the cocultivation (posttreat), and the conditions of administration are denoted below each **column**. Pretreatment with IL10 markedly increased the efficiency of cardiomyogenesis; progesterone, modestly, but significantly, increased the efficiency. **C,** IL10-induced increase in the cardiomyogenic transdifferentiation efficiency was significantly attenuated by the administration with FK506 or hydrocortisone (COR). **D,** IL10-induced increase in cardiomyogenic transdifferentiation efficiency was completely blocked by the administration of anti HLA-G antibody and anti-IL10 antibody.

(Figure 5B) by immunohistochemical analysis. There was no correlation between continuous secretion of the soluble HLA-G in the sera (ELISA) and survival of hAMC-derived cardiomyocytes (Figure 5C). On the other hand, adjacent to the surviving hAMC-derived cardiomyocytes, FOXP3-positive regulatory T cells were constantly detected by immunohistochemistry (Figure 5D and 5E; Online Figure IX), whereas they were not detected in control myocardium. The effects of IL10 or progesterone on the HLA-G expression in hAMCs were examined. Western blot analysis showed that IL10 and progesterone increased the HLA-G expression (Figure 5F). Concordantly, pretreatment with IL10 or progesterone before the hAMC transplantation significantly increased the incidence of survival of EGFP-positive hAMC-derived cardiomyocytes in vivo (Figure 5G).

Furthermore, the effect of IL10 or progesterone on the cardiomyogenic transdifferentiation efficiency of hAMCs was examined. IL10 or progesterone was administrated to the hAMCs (PDs=13) before and/or after the cardiomyogenic induction, then cardiomyogenic transdifferentiation efficiency was measured (Figure 6A and 6B). Surprisingly, both IL10 and progesterone significantly improved cardiomyogenic transdifferentiation efficiency in vitro. It is notable that pretreatment with IL10 or progesterone before cardiomyogenic induction is essential for this increase in cardiomyogenic transdifferentiation efficiency. Administration of FK506 and hydrocortisone significantly attenuated the IL10-induced increase in cardiomyogenic transdifferentiation efficiency (Figure 6C) in vitro. Moreover, the effect of IL10 was completely blocked by either anti IL10 antibody or anti HLA-G antibody administration (Figure 6D).

Discussion

We isolated hAMCs in the present study. Our isolated hAMCs can be transdifferentiated into cardiomyocytes in vitro and vivo, without using any epigenetic agent or gene transfer. The cardiomyogenic transdifferentiation efficiency of hAMCs was significantly higher than that of marrow-derived mesenchymal stem cells. Furthermore, xenografted hAMCs transdifferentiated into cardiomyocytes and survived more than 2 weeks (observed up to 80 days; Online Figure V); this suggests hAMCs were tolerated in situ. Immunologic

Downloaded from circres.ahajournals.org at KEIO UNIV IGAKUBU LIB on March 15, 2011

tolerance and cardiomyogenic transdifferentiation of hAMCs were significantly increased by pretreatment with IL10 or progesterone. From these findings, we concluded hAMCs can be a ready-to-use allograftable cellular source for cardiac stem cell therapy.

Highly Cardiomyogenic Transdifferentiation of hAMCs

The cardiomyogenic transdifferentiation efficiency of hAMCs at PD4 was calculated as 33%, which is higher than that of PCPCs.[9] Moreover, hAMCs express OCT-4 and SSEA4, a stem cell marker, and have a potential to differentiate into endodermal, mesodermal, and ectodermal lineage (Online Figure X) to some extent. These findings indicate that hAMCs have a ability to transdifferentiate into cells of various organs in comparison to other human somatic stem cells. This potential may contribute to the high cardiomyogenic transdifferentiation ability of hAMCs. The surface marker analysis clearly showed hAMCs have a mesenchymal phenotype. Despite a lack of expression of Nkx 2.5, a cardiac homeobox gene for cardiac differentiation, several cardiomyocyte-specific genes were expressed at the default state of hAMCs. Histological and physiological examinations revealed that hAMCs transdifferentiated into matured and physiologically functioning cardiomyocytes in vitro and in vivo. Moreover, transplantation of hAMCs improved cardiac functions and reduced the area of MI in vivo. The hAMCs-derived cardiomyocytes may play a role in improvement of cardiac function; however, antiapoptotic effect[24] of hAMCs may play a significant role in the present study. In the present study, neovascularization[25,26] may not play a major role in the improvement because hAMCs did not affect the capillary density (Online Figure XI).

Evidence of Tolerance

Tolerance is extremely important for clinical application of hAMCs, because we can use enormous numbers of hAMCs obtained from every delivery without establishing a stem cell bank system to match host and donor HLA-types. It is also notable that massive numbers of hAMC-derived cardiomyocytes were tolerated and survived in the xenografted host heart without using an immunosuppressant.

It is common that either allografted or xenografted cells could not survive for more than 2 weeks in the immunocompetent hosts because of rejection by the host's immune system. Therefore, massive survival of transdifferentiated EGFP-positive hAMCs in the Wistar rat heart for more than 2 weeks strongly suggests tolerance. Two independent FISH analysis clearly support the conclusion that the isolated EGFP-positive cardiomyocytes are of hAMC origin (have human nuclei) and are evidence of tolerance in the host heart.

The Mechanism of Tolerance

Because placenta and amniotic membrane are known to play an important role in avoiding maternal immunologic rejection against the fetal tissue bearing paternal alloantigens during normal gestation, it may be possible that the engrafted hAMCs were immunologically tolerated in the host heart. In comparison to other mesenchymal cells, hAMCs express lower MHC antigens; this might have importance for inducing tolerance in the host, because xenografted MMCs,[7] which express HLA-G and HLA-ABC, were completely rejected (n=4, data not shown). The expression pattern of HLAs suggests that hAMCs are resistant to MHC-dependent rejection mediated by T cell immune systems, but are known to be rejected by substitutive mechanisms. Cells that do not express the MHC molecule may be recognized as missing self cells, and may be attacked by natural killer cells.[27]

The nonclassic MHC class I antigen HLA-G expressed on the extravillous cytotrophoblast cells at the fetomaternal interface, is thought to play a major role in protecting the fetus from maternal rejection by natural killer cells.[28] Furthermore, HLA-G blocks the immunologic response of natural killer cells[29] and induces regulatory T cells,[30] which play an important role in immunologic tolerance.[31–33] In the present study, despite the fact that hAMCs expressed HLA-G in vitro, there is no correlation between the survival of EGFP-positive cardiomyocytes and continuous secretion of sHLA-G/HLA-G in Wistar rats in vivo. From these findings we speculated that HLA-G might play a role in the initial process of tolerance; however, it may not play a major role in tolerance maintenance.

A previous report showed that HLA-G–induced regulatory T cells, defined as FOXP3 positive lymphocytes,[30] also play a significant role in tolerance maintenance. Emergence and mobilization of FOXP3-positive lymphocytes beside the survived EGFP-positive cardiomyocytes in the present study strongly suggest that the regulatory T cell also plays an important role in maintenance of immunologic tolerance. However, it is difficult to verify this hypothesis by observing survival of hAMC-derived cardiomyocytes to evaluate tolerance, because the blockade of HLA-G must inhibit cardiomyogenic transdifferentiation efficiency in vivo. Because both tolerance and transdifferentiation efficiency increase the number of hAMC-derived cardiomyocytes in vivo, it is difficult to demonstrate direct evidence for the role of HLA-G in tolerance by simply determining the number of hAMC-derived cardiomyocytes. Further experimentation should be performed.

IL10, known as an immunosuppressive cytokine, is produced by regulatory T cells and type 2 helper T cells.[34,35] Progesterone and IL10, which are known to play an important role in causing fetomaternal immunologic tolerance and maintenance of normal pregnancy,[32,36,37] dramatically increase the HLA-G secretion from hAMCs. Concordant with the degree of HLA-G expression, the pretreatment of hAMCs with IL10 significantly increased the survival rate of EGFP-positive cardiomyocytes in Wistar rat hearts. This also suggested the major role of HLA-G in immunologic tolerance in the present study.

Relation Between the Immunologic Reaction and Cardiomyogenic Transdifferentiation of hAMCs

The mechanism of cardiac transdifferentiation of hAMCs is still undetermined; however, it is notable that the immunosuppressive cytokine IL10, or progesterone, dramatically increased the cardiomyogenic transdifferentiation efficiency, whereas FK506 or hydrocortisone attenuated the efficiency. This finding was also associated with the fact that mesenchymal cells, having significant cardiomyogenic transdifferentiation ability, can be obtained from gestation-related organs, ie, umbilical cord blood,[8] uterine endometrium,[7] menstrual

Downloaded from circres.ahajournals.org at KEIO UNIV IGAKUBU LIB on March 15, 2011